537

Applications of Satellite Remote Sensing

A dissertation submitted to the Department of Physics, Quaid-i-Azam University, Islamabad, in the partial fulfillment of the requirement for the degree of

Master of Philosophy
In Physics

By

Muhammad Asif

DEPARTMENT OF PHYSICS

QUAID-I-AZAM UNIVERSITY

ISLAMABAD

2002

Dedicated to

The

AFFECTION

of

My Parents
and to
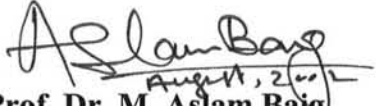Brothers & Sister
who always encouraged me

CERTIFICATE

This is certified that the experimental work in this dissertation has been carried out by *Mr. Muahmmad Asif* under my supervision, in close collaboration with SUPARCO Satellite Ground Station, Islamabad and is accepted in its present form by the Department of Physics, Quaid-i-Azam University, Islamabad, as satisfying the dissertation requirement for the degree of Master of Philosophy in Physics.

Prof. Dr. M. Aslam Baig

Supervisor

Department of Physics
Quaid-i-Azam University
Islamabad

Submitted through

Prof. Dr. Asghari Maqsood

Chairperson

Department of Physics
Quaid-i-Azam University
Islamabad.

Acknowledgements

All praise to Almighty Allah who created all beings and this symmetric, harmonious and thought provoking Universe and great respects for the Holy Prophet Muhammad (Sallallaho Alaihe Wasallam) who enabled us to recognize our creator.

I find no words to express my sincere gratitude for Prof. Dr. M. Aslam Baig, my honorable teacher and research supervisor, who was very affectionate and cooperative during this research work and all other times. His guidance and personal interest was major encouraging factor for me. My deep appreciations to Prof. Dr. Asghari Maqsood, Chairperson of the Department of Physics for providing the research facilities.

I am greatly indebted to Mr. Ejaz Ahmad Bhutta, Muhammad Iftikhar Bhatti, Tariq Masood, Muhammad Yasin Bassam Waheed and Waqar Ahmad for their kind help and useful suggestions during this work. I am also grateful to all my lab fellows Anwar, Aysha, Perveen, and Hidyat Ullah.

I am obliged to all my friends, Aqeel Ahsan Khuram, Sajid Hussain, Iftikhar Hussain Gul, Muhammad Shafi, Tahir Khalil Ahsan and Muhammad Uzair for their useful discussions and sincere cooperation during my research.

My special thanks are due for SUPARCO Satellite Ground Station, Islamabad for their cooperation during this work.

Lastly but whole heartedly, I pay my gratitude to my brothers and the dearest sister for their prayers and moral support.

Muhammad Asif

ABSTRACT

Integration of Satellite Remote Sensing (SRS) and Geographic Information Systems (GIS) is a useful tool for monitoring natural resources. This project deals with the monitoring of siltation effects, forest change detection and environmental impact assessments in the precincts of Mangla Dam after increasing the proposed height of dam by using the Satellite Remote Sensing and GIS techniques. A large amount of sediments have deposited in the dam due to which its storage capacity is decreasing gradually, hence an aspect is under consideration that, is it feasible to increase the height of Mangla dam? to enhance the storage capacity of reservoir. Proposed increase in height of dam is 40 feet. Digital image data of SPOT satellite system and Landsat TM with 20m and 30m spatial resolution respectively, has used for this purpose. The data were geo-rectified using Survey of Pakistan (SoP) reference maps. From the rectified and processed satellite image different objects e.g. Reservoir boundary, Forests, Rivers, Drainage (includes small water tributaries, streams and Nallahs), Residential Area and road network have been identified, marked and digitized. Digital Elevation Model (DEM) of Mangla Reservoir area was generated from contour lines, using GIS techniques. From this DEM the Digital Terrain Model (DTM) and 3D grid of Mangla dam's reservoir area was generated for better understanding of the terrain. The interfacing of GIS, DEM and SRS provided a new and exciting capability to analyze the dynamics of land-use change and to assess changes in residential areas and vegetation in the landscape after raising the Dam's height. After analysis it is concluded that some of residential areas, different parts of the forests and reservoir surrounding land will go underwater. This increase in height of dam will affect about 40,000 people. In spite of all these, this will increase the storage capacity of Mangla reservoir up to 3.1 million acres feet and 18% more electricity will be also generated.

<u>Contents</u>

Chapter # 3
CASE STUDY

Chapter 1

AN INTRODUCTION TO SATELLITE REMOTE SENSING

1.1   The Concept of Remote Sensing

We have heard the term "remote sensing" before. But, just what does it mean? It's a fancy phrase for a concept that is rather simple and certainly familiar. As we scrutinize the screen of our video monitor, we are actively engaged in remote sensing.

Something physical - light - is emanating from that screen - a source of radiation - which passes over a distance - and thus is "remote" to some extent - until it encounters and is captured by a sensor - our eyes - which then sends a signal to a processor - our brain. The human senses gather their awareness of the external world almost entirely by perceiving a variety of signals, either emitted or reflected, actively or passively, from objects that transmit this information in the form of waves or pulses.

A formal and comprehensive definition of applied remote sensing, as it is customarily given, is:

Remote Sensing is the observation of a target by a device separated from it by some distance, in contrast to in situ sensing where measuring device are immersed in, or at least touch, the object of measurement [4].

Remote Sensing is defined as the science and technology by which the characteristics of objects of interest can be identified, measured or analyzed the characteristics without direct contact [4].

The science and art of obtaining useful information about an object, area or phenomenon through the analysis and interpretation of image data acquired by a device that is not in contact with the object, area or phenomenon under investigations [3].

The acquisition and measurement of data/information on some property(ies) of a phenomenon, object, or material by a recording device not in physical, intimate contact with the feature(s) under surveillance; techniques involve amassing knowledge pertinent to environments by measuring force fields, electromagnetic radiation, or acoustic energy employing cameras, lasers, radio frequency receivers, radar systems, sonar, thermal devices, seismographs, magnetometers, gravimeters, scintillometers, and other instruments [1].

This is a rather lengthy and all-inclusive definition. Perhaps a simplified definition is in order:

Remote Sensing is a technology based on sampling radiation and force fields that seeks to acquire and interpret geospatial data to develop information about features, objects, and classes on the Earth's land surface, oceans, and atmosphere (and where applicable on the exterior's of other planets) [2].

Or the variation:

1

Remote Sensing involves the detection and measurement of photons of differing energies emanating from distant materials, by which these may be identified and categorized by class/type, substance, and spatial distribution [1].

All of these statements are valid and, taken together, give us a reasonable insight into the meaning and use of the phrase or term *"Remote Sensing"*.

1.2   Types of Remote Sensing with Respect to Wavelength Regions

Remote sensing is classified into three types with respect to the wavelength regions;

as shown in Figure 1.1

1.2.1 Visible and Reflective Infrared Remote Sensing

The energy source used in the visible and reflective infrared remote sensing is the sun. The sun radiates electro-magnetic energy with a peak wavelength of 0.5 μm. Remote sensing data obtained in the visible and reflective infrared regions mainly depends on the reflectance of objects on the ground surface. Therefore, information about objects can be obtained from the spectral reflectance. However laser radar is exceptional because it does not use the solar energy but the laser energy of the sensor.

1.2.2 Thermal Infrared Remote Sensing

The source of radiant energy used in thermal infrared remote sensing is the object itself, because any object with a normal temperature will emit electro-magnetic radiation with a peak at about 10 μm, as illustrated in Figure 1.1

One can compare the difference of spectral radiance between the sun (a) and an object with normal earth temperature (about 300°K), as shown in Figure 1.1. However it should be noted that the figure neglects atmospheric absorption, for simplification, though the spectral curve varies with respect to the reflectance, emittance and temperature of the object. The curves of (a) and (b) cross at about 3.0 μm. Therefore in the wavelength region shorter than 3.0 μm, spectral reflectance is mainly observed, while in the region longer than 3.0 μm, thermal radiation is measured.

The two curves (a) and (b) in Figure 1.1 show the black body's spectral radiances of the sun at a temperature of 6,000°K and an object with a temperature of 300°K, without atmospheric absorption.

1.2.3 Microwave Remote Sensing

In the microwave region, there are two types of micro wave remote sensing, passive microwave remote sensing and active microwave remote sensing. In passive microwave
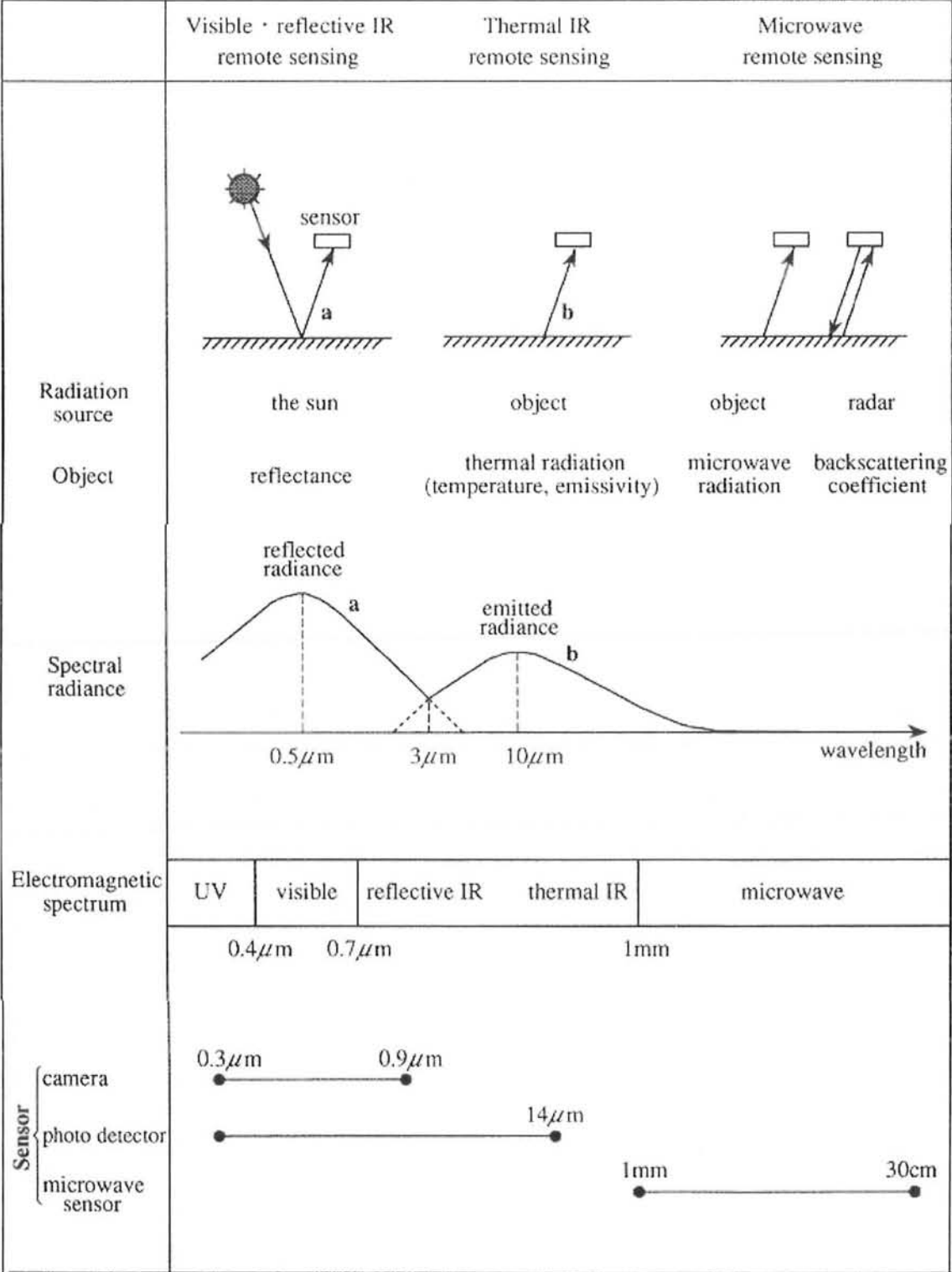
Figure1.1: Types of Remote Sensing with Respect to Wavelength Regions

remote sensing, the microwave radiation emitted from an object is detected, while the back scattering coefficient is detected in active micro wave remote sensing.

1.3   Reflectance

Reflectance is defined as the ratio of incident flux on a sample surface to reflected flux from the surface. Reflectance ranges from 0 to 1. Reflectance was originally defined as a ratio of incident flux of white light to reflected flux in a hemisphere direction. Reflectance with respect to wavelength is called spectral reflectance. A basic assumption in remote sensing is that spectral reflectance is unique and different from one object to an other object.

Reflectance with a specified incident and reflected direction of electro-magnetic radiation or light is called directional reflectance. The two directions of incident and reflection can be directional, conical or hemispherical making nine possible combinations.

For example, if incident and reflection are both directional, such reflectance is called bidirectional reflectance. The concept of bidirectional reflectance is used in the design of sensors.

A perfectly diffuse surface is defined as a uniformly diffuse surface with a reflectance of 1, while the uniformly diffused surface, called a Lambertian surface, reflects a constant radiance regardless of look angle.

The Lambert cosine law which defines a Lambertian surface is as follows:

$$I(\theta) = I_n \cos \theta$$

where $I(\theta)$: luminous intensity at an angle of θ from the normal to the surface. I_n : luminous intensity at the normal angle

1.3.1 Spectral Reflectance of Land Covers

Spectral reflectance is assumed to be different with respect to the type of land cover, as explained earlier. This is the principle that in many cases allows the identification of land covers with remote sensing by observing the spectral reflectance or spectral radiance from a distance far removed from the surface.

Figure 1.2(a) shows three curves of spectral reflectance for typical land covers; vegetation, soil and water. As seen in the figure, vegetation has a very high reflectance in the near infrared region, though there are three low minima due to absorption.

Soil has rather higher values for almost all spectral regions. Water has almost no reflectance in the infrared region.

Figure 1.2(b) shows two detailed curves of leaf reflectance and water absorption. Chlorophyll, contained in a leaf, has strong absorption at 0.45 μm and 0.67 μm, and high reflectance at near infrared (0.7-0.9 μm). This results in a small peak at 0.5-0.6 (green color band), which makes vegetation green to the human observer.

Near infrared is very useful for vegetation surveys and mapping because such a steep gradient at 0.7-0.9 μm is produced only by vegetation.

Because of the water content in a leaf, there are two absorption bands at about 1.5 μm and 1.9 μm. This is also used for surveying vegetation vigor.

Figure 1.2(c) shows a comparison of spectral reflectance among different species of vegetation.

Figure 1.2(d) shows various patterns of spectral reflectance with respect to different rock types in the short wave infrared (1.3-3.0 μm). In order to classify such rock types with different narrow bands of absorption, a multi-band sensor with a narrow wavelength interval is to be developed. Imaging spectrometers have been developed for rock type classification and ocean color mapping.

1.4   Transmittance of the Atmosphere

The sunlight's transmission through the atmosphere is affected by absorption and scattering of atmospheric molecules and aerosols. The reduction of sunlight intensity is called extinction. The rate of extinction is expressed as extinction coefficient.

The optical thickness of the atmosphere corresponds to the integrated value of the extinction coefficient at each altitude by the atmospheric thickness. The optical thickness indicates the magnitude of absorption and scattering of the sunlight. The following elements will influence the transmittance of the atmosphere.

a. Atmospheric molecules(smaller size than wavelength):
carbon dioxide, ozone, nitrogen gas, and other molecules

b. Aerosols (larger size than wavelength):
water drops such as fog and haze, smog, dust and other particles with a bigger size
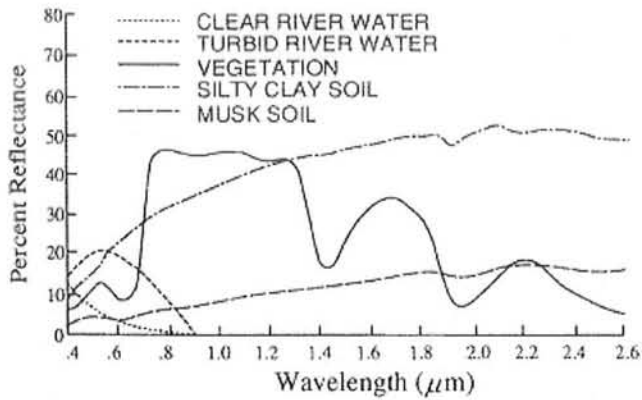
Figure: a)
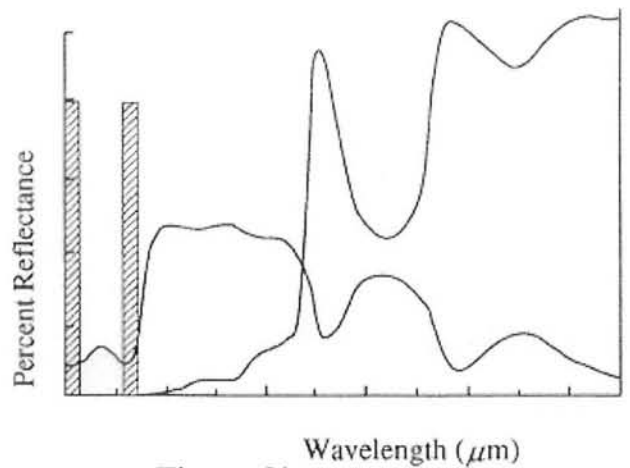
Figure: b)
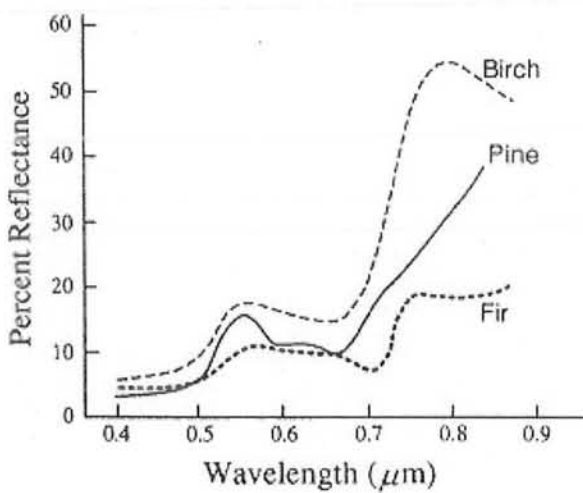
Figure: c)
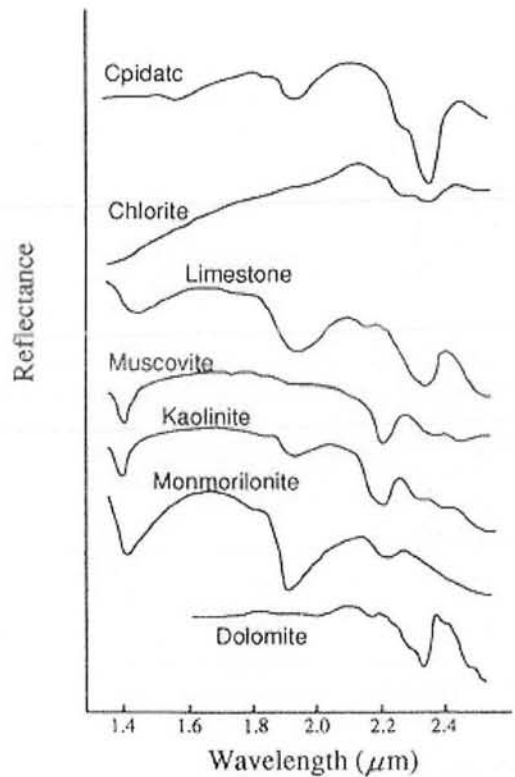
Figure: d)

Figure1.2*: Spectral reflectance of some land covers
   a) Spectral reflectance of vegetation, soil and water
   b) Spectral reflectance of green leaf
   c) Spectral reflectance of different kinds of plants
   d) Spectral reflectance of rocks and minerals

* Ref: Guneriussen, T. and H. Johnsen *"NASDA Remote Sensing Tutorials"*.

Scattering by atmospheric molecules with a smaller size than the wavelength of the sunlight is called "Rayleigh scattering". Raleigh scattering is inversely proportional to the fourth power of the wavelength.

The contribution of atmospheric molecules to the optical thickness is almost constant spatially and with time, although it varies somewhat depending on the season and the latitude.

Scattering by aerosols with larger size than the wavelength of the sunlight is called "Mie scattering". The source of aerosols will be suspended particles such as sea water or dust in the atmosphere blown from the sea or the ground, urban garbage, industrial smoke, volcanic ashes etc., which varies to a great extent depending upon the location and the time. In addition, the optical characteristics and the size distribution also changes with respect to humidity, temperature and other environmental conditions. This makes it difficult to measure the effect of aerosol scattering.

Scattering, absorption and transmittance of the atmosphere are different for different wavelengths. The open region with higher transmittance in called "an atmospheric window".

As the transmittance partially includes the effect of scattering, the contribution of scattering is larger in the shorter wavelengths. The contribution by scattering is dominant in the region less than 2mm and proportional according to the shorter wavelength. The contribution by absorption is not constant but depends on the specific wavelength.

1.5   Sensor

Device that receives electromagnetic radiation and converts it into a signal that can be recorded and displayed as either numerical data or an image[1].

Or

*A device to detect the electro-magnetic radiation reflected or emitted from an object is called a "remote sensor" or "**sensor**". Cameras or scanners are examples of remote sensors*[2].

1.5.1   Types of Sensor

Figure 1.3 summarizes the types of sensors now used or being developed in remote sensing. Passive sensors detect the reflected or emitted electro-magnetic radiation from natural sources, while active sensors detect reflected responses from objects which are irradiated from artificially generated energy sources, such as radar.Each is divided further in to non-scanning and scanning systems. A sensor classified as a combination of passive, non-scanning and non-imaging method is a type of profile recorder, for example a microwave radiometer. A sensor classified as passive, non-scanning and imaging method, is a camera, such as an aerial survey camera or a space camera, Sensors classified as a combination of passive, scanning and imaging are classified further into image plane scanning sensors, such as TV cameras and solid state scanners, and object plane scanning sensors, such as multispectral scanners (optical-mechanical scanner) and scanning microwave radiometers.

The most popular sensors used in remote sensing are the camera, solid state scanner, such as the CCD (charge coupled device) images, the multi-spectral scanner and in the future the passive synthetic aperture radar.

Those sensors which use lenses in the visible and reflective infrared region, are called optical sensors.

1.6   Characteristics of Optical Sensors

Optical sensors are characterized specified by spectral, radiometric and geometric performance. Figure 1.4 summarizes the related elements for the three characteristics of optical sensor.

1.6.1   Spectral characteristics

The spectral characteristics are spectral band and band width, the central wavelength,

Sensor

Passive
  Non-Scanning
    Non-Imaging
      - Microwave Radiometer
      - Magnetic sensor
      - Gravimeter
      - Fourier Spectrometer
      - Others
    Imaging — Camera
      - Monochrome
      - Natural Color
      - Infrared
      - Color Infrared
      - Others
  Scanning — Imaging
    Image Plane Scanning
      - TV Camera
      - Solid Scanner
    Object Plane Scanning
      - Optical Mechanical Scanner
      - Microwave Radiometer

Active
  Non-Scanning — Non-Imaging
    - Microwave Radiometer
    - Microwave Altimeter
    - Laser Water Depth Meter
    - Laser Distance Meter
  Scanning — Imaging
    Object Plane Scanning
      - Real Aperture Radar
      - Synthetic Aperture Radar
    Image Plane Scanning
      - Passive Phased Array Radar

Figure1.3: Types of sensors

Sensor
  — Spectral characteristics
      — observation range of EMW
      — changes at both ends of a band
      — sensitivity on out of a band
      — polarization sensitivity
      — sensitivity different between different bands
        ⋮
  — Radiometric characteristics
      — detecting accuracy
      — signal to noise ratio
      — dynamic range
      — quantization level
      — sensitivity difference between pixels
      — linearity of sensitivity
      — noise equivalent power
        ⋮
  — Geometric characteristics
      — field of view
      — instantaneous field of view
      — registration between different spectral bands
      — alignments
      — MTF
      — optical distortion
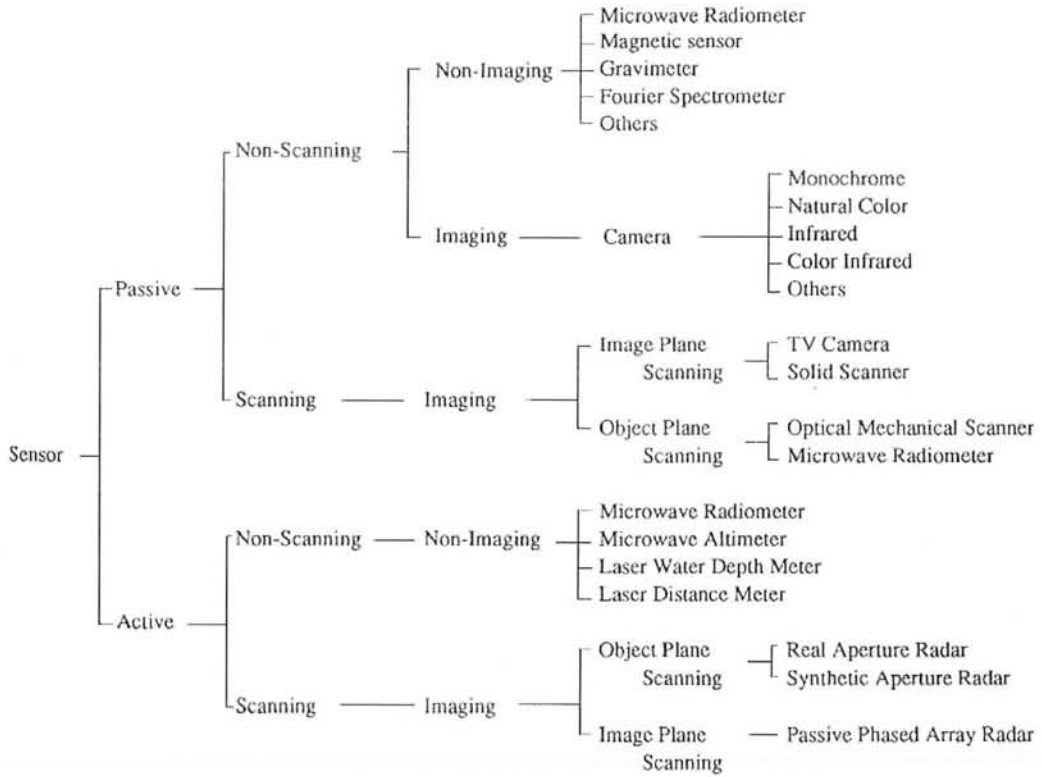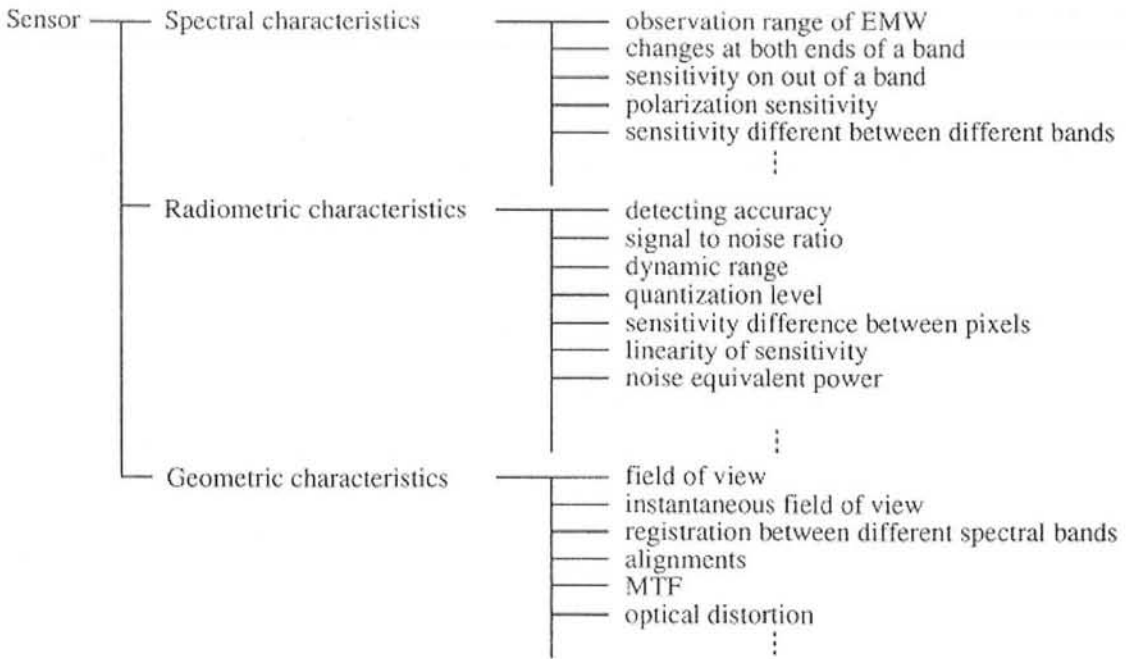   ⋮

Figure1.4: Characteristics of Optical Sensors

9

response sensitivity at the edges of band, spectral sensitivity at outer wavelengths and sensitivity of polarization.

1.6.2 Radiometric characteristics

Sensors using film are characterized by the sensitivity of film and the transmittance of the filter, and nature of the lens. Scanner type sensors are specified by the spectral characteristics of the detector and the spectral splitter. In addition, chromatic aberration is an influential factor. The radiometric characteristics of optical sensors are specified by the change of electro-magnetic radiation which passes through an optical system. They are radiometry of the sensor, sensitivity in noise equivalent power, dynamic range, signal to noise ratio (S/N ratio) and other noises, including quantification noise.

1.6.3 Geometric characteristics

The geometric characteristics are specified by those geometric factors such as field of view (FOV), instantaneous field of view (IFOV), band to band registration, MTF geometric distortion and alignment of optical elements.

IFOV is defined as the angle contained by the minimum area that can be detected by a scanner type sensor(see fig). For example in the case of an IFOV of 2.5 milli radians, the detected area on the ground will be 2.5 meters x 2.5 meters,if the altitude of sensor is 1,000 m above ground.

1.7 Optical Mechanical Scanner

An optical mechanical scanner is a multispectral radiometer by which two dimensional imagery can be recorded using a combination of the motion of the platform and a rotating or oscillating mirror scanning perpendicular to the flight direction. Optical mechanical scanners are composed of an optical system, spectrographic system, scanning system, detector system and reference system.

Optical mechanical scanners can be carried on polar orbit satellites or aircraft. Multispectral scanner (MSS) and thematic mapper (TM) of LANDSAT, and Advanced Very High Resolution Radiometer (AVHRR) of NOAA are the examples of optical mechanical scanners. M2S made by Daedalus Company is an example of an airborne type optical mechanical scanner.

Figure 1.5 shows the concept of optical mechanical scanners, while Figure 1.6 shows a schematic diagram of the optical process of an optical mechanical scanner.
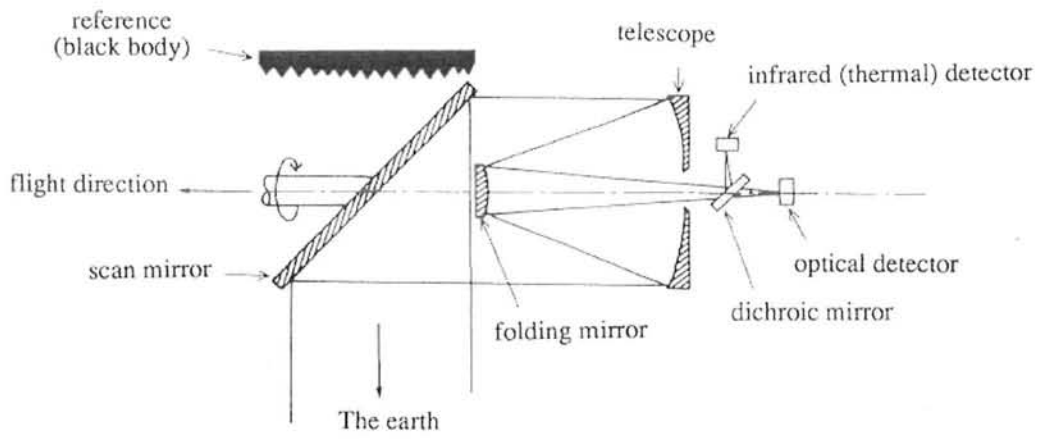
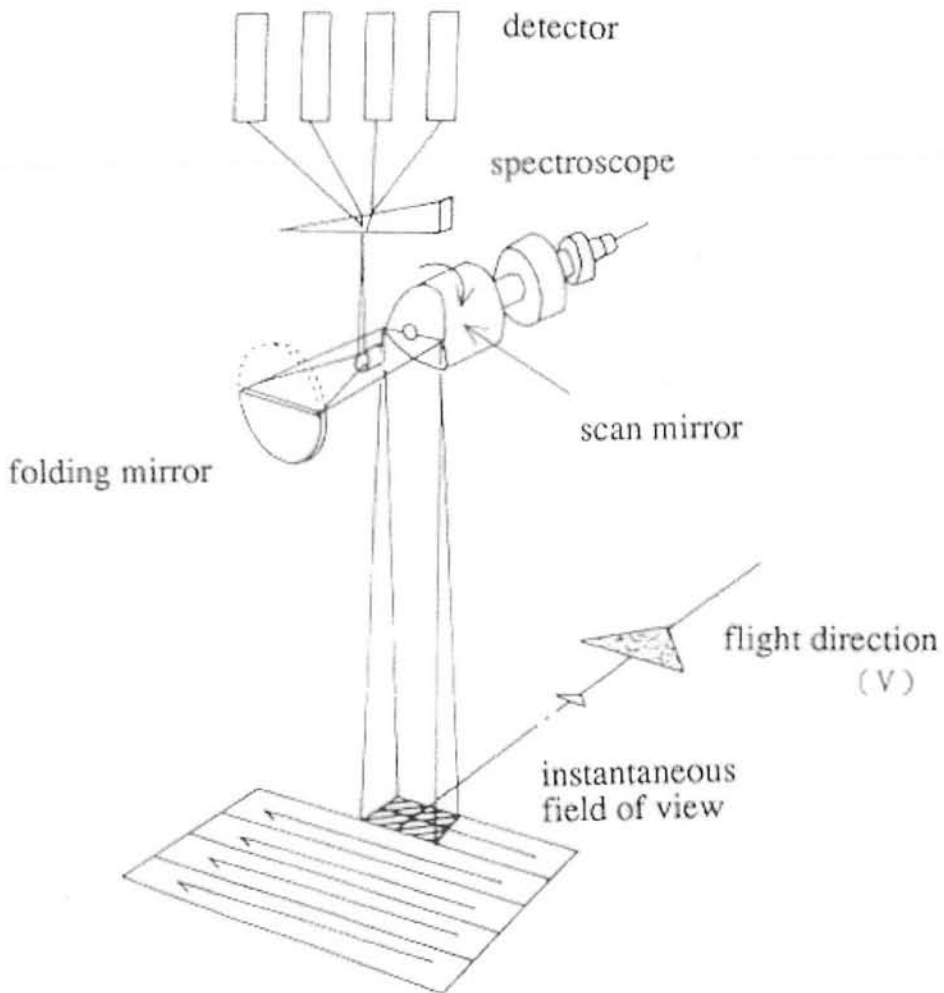**Figure1.5**: Structure of optical mechanical scanner

Figure1.6: Schematic of optical mechanical scanner

11

The function of the elements of an optical mechanical scanner are as follows

a. Optical system: Reflective telescope system such as Newton, Cassegrain or Ritchey-Chretien is used to avoid color aberration.

b. Spectrographic system: Dichroic mirror, grating, prism or filter are utilized.

c. Scanning system: rotating mirror or oscillating mirror is used for scanning perpendicular to the flight direction.

d. Detector system: Electro magnetic energy is converted to an electric signal by the optical electronic detectors. Photomultiplier detectors utilized in the near ultra violet and visible region, silicon diode in the visible and near infrared, cooled ingium antimony (InSb) in the short wave infrared, and thermal barometer or cooled Hq Cd Te in the thermal infrared.

e. Reference system: The converted electric signal is influenced by a change of sensitivity of the detector. Therefore light sources or thermal sources with constant intensity or temperature should be installed as a reference for calibration of the electric signal.

Compared to the pushbroom scanner, the optical mechanical scanner has certain advantages. For examples, the view angle of the optical system can be very narrow, band to band registration error is small and resolution is higher, while it has the disadvantage that signal to noise ratio (S/N) is rather less because the integration time at the optical detector cannot be very long due to the scanner motion.

1.7.1   Landsat: The Thematic Mapper

A more sophistical multispectral imaging sensor, named the Thematic Mapper (TM) has been added to Landsats 4 (1982), 5 (1984), and 6 (the latter failed to attain orbit during launch and thus has never returned data). These flew on a redesigned, more advanced platform. Although similar in operational modes to the MSS (which was also part of the 4 and 5 payload, to maintain continuity), the TM consists of 7 bands that have these characteristics:

Band No.	Wavelength Interval (μm)	Spectral Response	Resolution (m)
1	0.45 - 0.52	Blue-Green	30
2	0.52 - 0.60	Green	30
3	0.63 - 0.69	Red	30
4	0.76 - 0.90	Near IR	30
5	1.55 - 1.75	Mid-IR	30
6	10.40 - 12.50	Thermal IR	120
7	2.08 - 2.35	Mid-IR	30

The six reflectance bands obtain their effective resolution at a nominal orbital altitude of 705 km (437 miles) through an IFOV of 0.043 mrad; the IFOV for the thermal channel is 0.172 mrad.

Band 1 is superior to MSS 4 in detecting some features in water; it also allows quasi-natural color composites to be put together. Band 5 is sensitive to variations in water content, both in leafy vegetation and as soil moisture; it also distinguishes between clouds (appearing dark) and bright snow (light). This band also responds to variations in ferric iron ($Fe_2 O_3$) content in rocks and soils, with materials containing this substance showing higher reflectances as its percentage increases. Band 7 likewise reacts to moisture contents and is especially suited to detecting hydrous minerals (such as clays or certain alteration products) in geologic settings. Band 6 can distinguish a radiant temperature difference of ~ 0.6 degrees C and is helpful in discriminating rock types whose thermal properties permit varying extents of heating and consequent differences in near surface temperatures; it often can pick out changes in ground temperatures due to moisture variation and can single out vegetation due to its evaporative cooling effect. The higher resolution achieved in the reflective bands is a significant aid in picking out features and classes whose minimum dimension is usually on the order of 30 m (100 ft) . Thus, houses and smaller buildings, which were unresolvable in MSS images, can often be discerned.

1.8   Pushbroom Scanner

The pushbroom scanner or linear array sensor is a scanner without any mechanical scanning mirror but with a linear array of solid semiconductive elements which enables it to record one line of an image simultaneously, as shown is Figure 1.7.

The pushbroom scanner has an optical lens through which a line image is detected simultaneously perpendicular to the flight direction. Though the optical mechanical scanner scans and records mechanically pixel by pixel, the pushbroom scanner scans and records electronically line by line. Because pushbroom scanners have no mechanical parts, their mechanical reliability can be very high. However, there will be some line noise because of sensitivity differences between the detecting elements.

Charge coupled devices, called CCD, are mostly adopted for linear array sensors. Therefore it is sometime called a linear CCD sensor or CCD camera. HRV of SPOT, MESSR of MOS-1, and OPS of JERS-1 are examples of linear CCD sensors as is the Itres CASI airborne system. As an example, MESSR of MOS-1 has 2048 elements with an interval of 14 mm. However CCD with 5,000 - 10,000 detector elements have been developed and available recently made available.

1.8.1   The SPOT Satellite

SPOT is an operational series of earth-observing satellites sponsored initially by the government of France and managed by the French Space Agency which, since the first
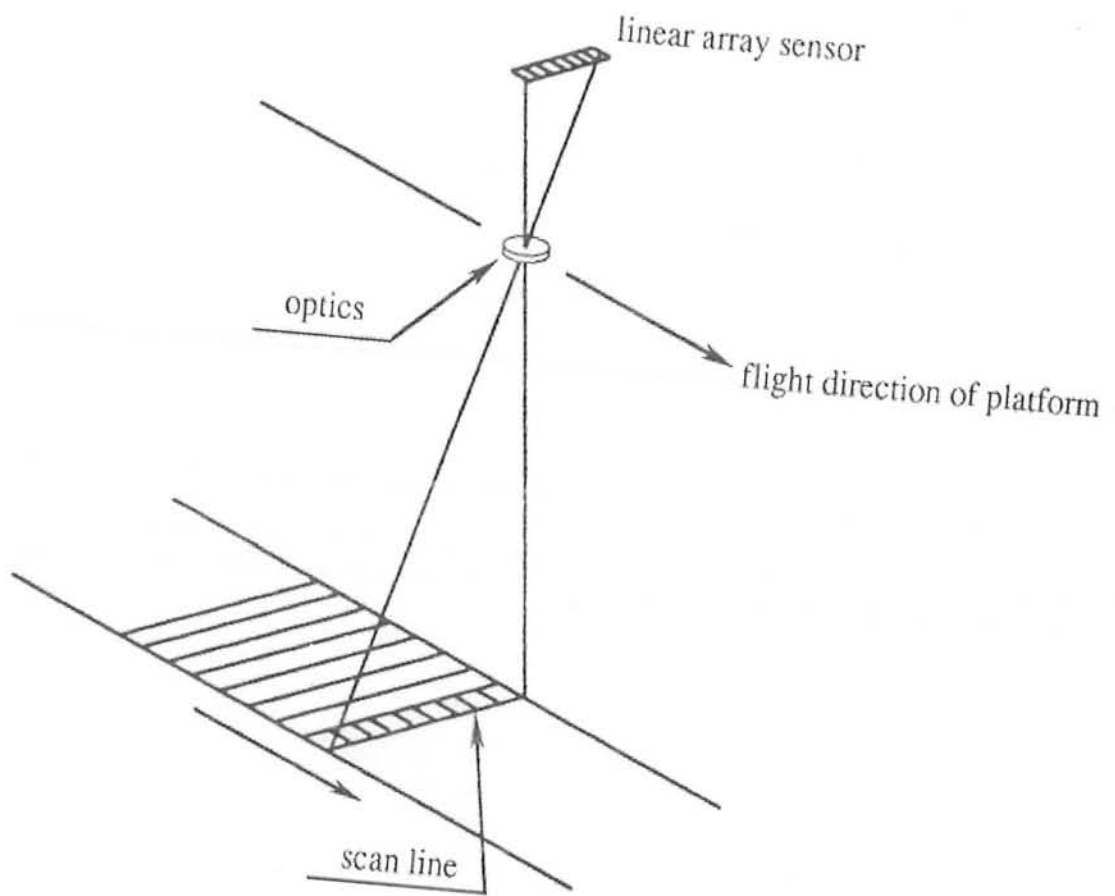
Figure1.7: Schematic diagram of data acquisition by
Push broom scanner

launch in 1986, is now offering multispectral data to world users on a commercial basis. From an 831 km (516 miles) sun-synchronous (10:30 A.M. equatorial crossing time), near polar orbital altitude, SPOT will revisit the same 117 kilometer wide ground tracks once every 26 days when its sensors are looking vertically downward (at nadir). However, its mirror can be moved sideways in both directions to view up to 27 degrees off-nadir, enabling it to examine areas within a 950 km-wide corridor astride its track path. With careful planning, and optimal cloud conditions, an area within this corridor can be revisited as many as 7 times during an orbital cycle. Images taken from different lateral angles on different dates can be paired such that their parallax offsets permit them to be viewed stereoscopically, thus facilitating a 3-D perspective of the ground surface of great value to topographic analysts, geomorphologists, and others.

The payload sensor on SPOT is known as the HRV (for High Resolution Visible). This is a slight misnomer, inasmuch as in its multispectral mode, Band 3 operates in the near-IR over the interval 0.79 - 0.89 µm (Band 1 = 0.50 - 0.59 µm [green] and Band 2 = 0.6 - 0.68 µm [red]). A separate unit in the HRV can also image in the panchromatic mode as a single band encompassing 0.51 - 0.70 µm. Instead of an oscillating scan mirror, the tilt able mirror (set either on or off-nadir) sends light to a linear array of tiny detectors (known as CCDs, for charged coupled devices; see p. I-13 for details on how these function), which receive photons simultaneously, that are very rapidly discharged in sequence into an electron current stream. This array is then reactivated by photons almost instantly as the array line moves to the next ground position along the forward track. In the panchromatic mode, there are 6000 detectors in the array, each receiving its light from a 10 x 10 m ground area, thus providing a resolution of 10 m for an image of 60 km (37 mile) width. The multispectral HRV contains 3000 detectors in the array, providing a ground resolution of 20 m. On the spacecraft there are two such HRV arrays, mounted side-by-side, each viewing its own 60 km swath width but the pair of images sidelapping to give an effective 117 km wide coverage.

Chapter 2

DIGITAL IMAGE PROCESSING

2.1   Digital Data

Images with a continuous gray tone or color, like a photograph are called analog images. On the other hand, a group of divided small cells, with integer values of average intensity, the center representing the cell's value, is called a digital image. The spatial division into a group of cells is called sampling as illustrated in Figure 2.1, while conversion of analog images into integer image data is called quantization as illustrated in Figure 2.2.

An individual divided cell is called a pixel (picture cell). The shape of the cell is usually square for easy use in a computer, though triangular or hexagonal can also be considered. A digital image has coordinates of pixel number, normally counted from left to right, and line number, normally counted from top to bottom.

The most important factor in sampling is pixel size or sampling frequency. If the pixel size is large or the sampling frequency is long, the appearance of the image becomes worse, while in the reverse case the data volume becomes very large. Therefore the optimum sampling should be carefully considered.

Shannon's sampling theorem, for specifying the optimum sampling, is given as follows.

"There will be no loss of information if sampling is taken with a half frequency of the maximum frequency involved in the original analog frequency wave."

The question is how to determine the number of quantization levels or the unit intensity as divider. If the number of levels is too small, the quantization error will increase. In the reverse, the data volume increases with informationless data because of the noise level. For example, the quantization should be divided by a level larger than that of the noise. In this example, four levels would be an appropriate quantization.

2.1.1   Geometric Characteristics of Image Data

Remote sensing data are data digitized by a process of sampling and quantization of the electro-magnetic energy which is detected by a sensor. In this section, geometric characteristics of sampling are described.

IFOV (Instantaneous Field Of View) is defined as the angle which corresponds to the sampling unit as shown in Figure 2.3. Information within an IFOV is represented by a pixel in the image plane.

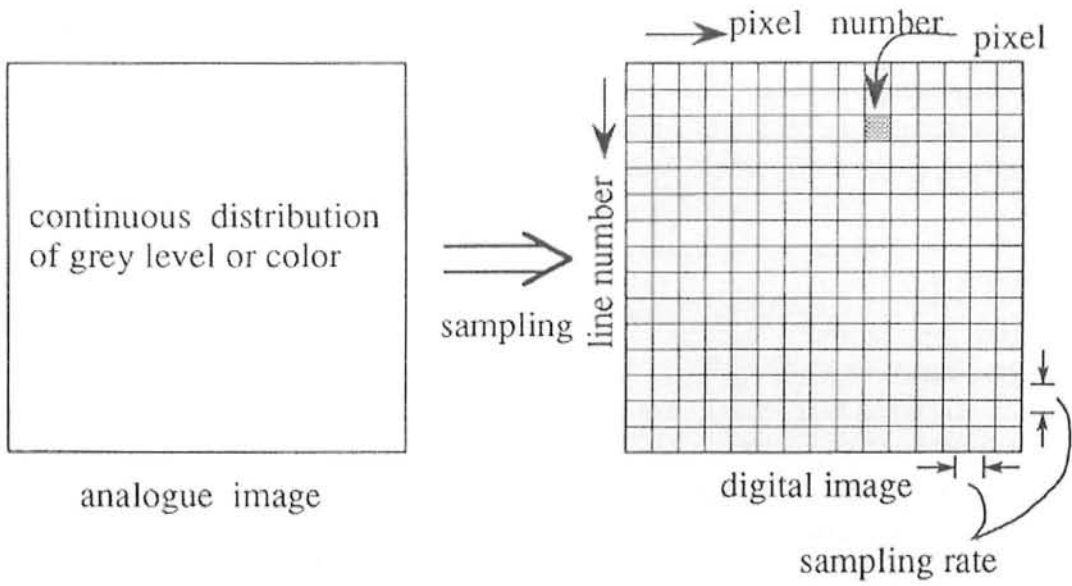**Figure2.1**: Concept of sampling

f : analogue intensity

f_d : quantized intensity

V : unit intensity

n : integer

$(n-0.5)V \leq f < (n+0.5)V \rightarrow f_d = n$

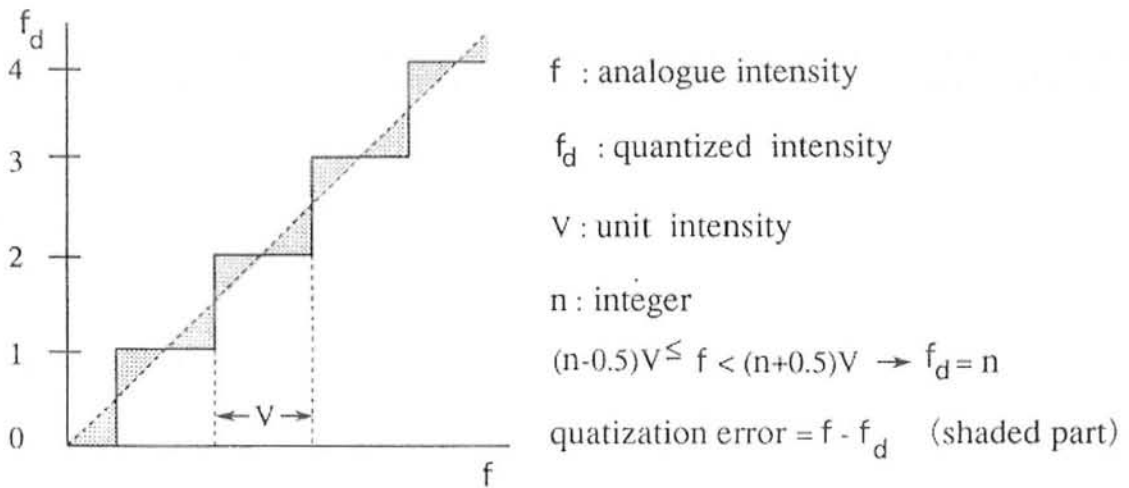quatization error = f - f_d (shaded part)

Figure2.2: Concept of quantization

The maximum angle of view which a sensor can effectively detect the electro magnetic energy, is called the FOV (Field Of View). The width on the ground corresponding to the FOV is called the swath width.

The minimum detectable area, or distance on the ground is called the ground resolution. Sometimes the projected area on the ground corresponding to a pixel or IFOV is also called the ground resolution.

In remote sensing, the data from a multiple number of channels or bands which divide the electromagnetic radiation range from Ultra Violet to Radio Waves are called multi-channel data, multi-band data or multi- spectral data.

In general, multi-channel data are obtained by different detectors as shown in Figure 2.4. Because the detectors are located at slightly different positions, and the light path of different wavelengths is a little different from each other, the images of multi-channel data are not identical in geometric position. To correct such geometric errors between channels is called registration.

2.1.2   Radiometric Characteristics of Image Data

Electromagnetic energy incident on a detector is converted to an electric signal and then digitized. In this quantization process, the relationship between the input signal and the output signal is generally represented.

One should be careful of the noise level in the case of quantization. The ratio of effective input signal S to the noise level N is called the S/N ratio (signal to noise ratio), which is given as follows.

$$S / N \text{ ratio} = 20 \log 10 \ (S/N) \ [dB]$$

Quantization is specified by the dynamic range and the S/N ratio. Information contained in digitized image data are expressed by bit (binary digit) per pixel per channel.

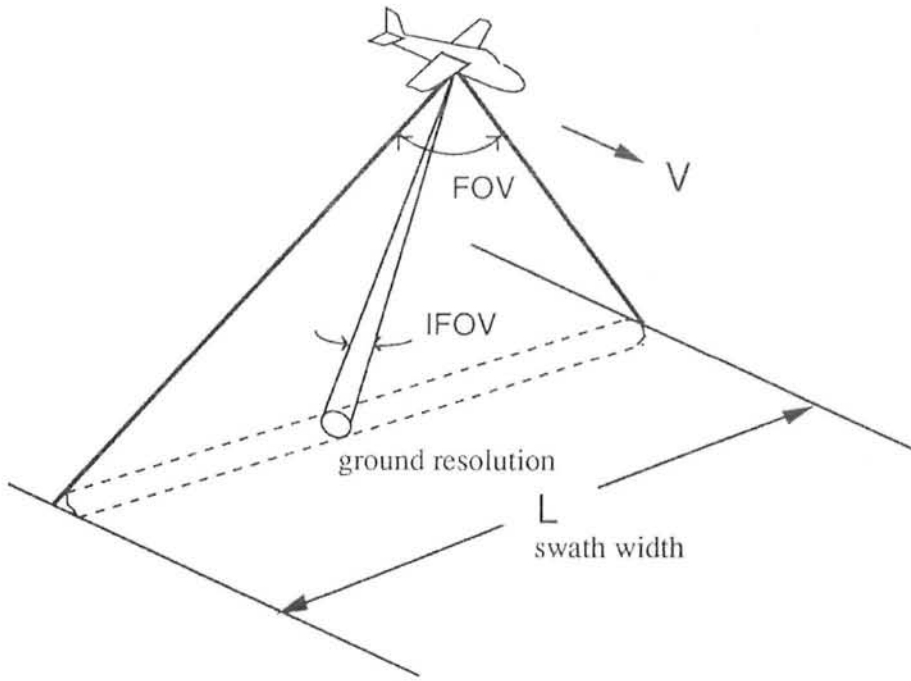A bit is a binary number that is 0 or 1. Let the quantization level be n, then the

18

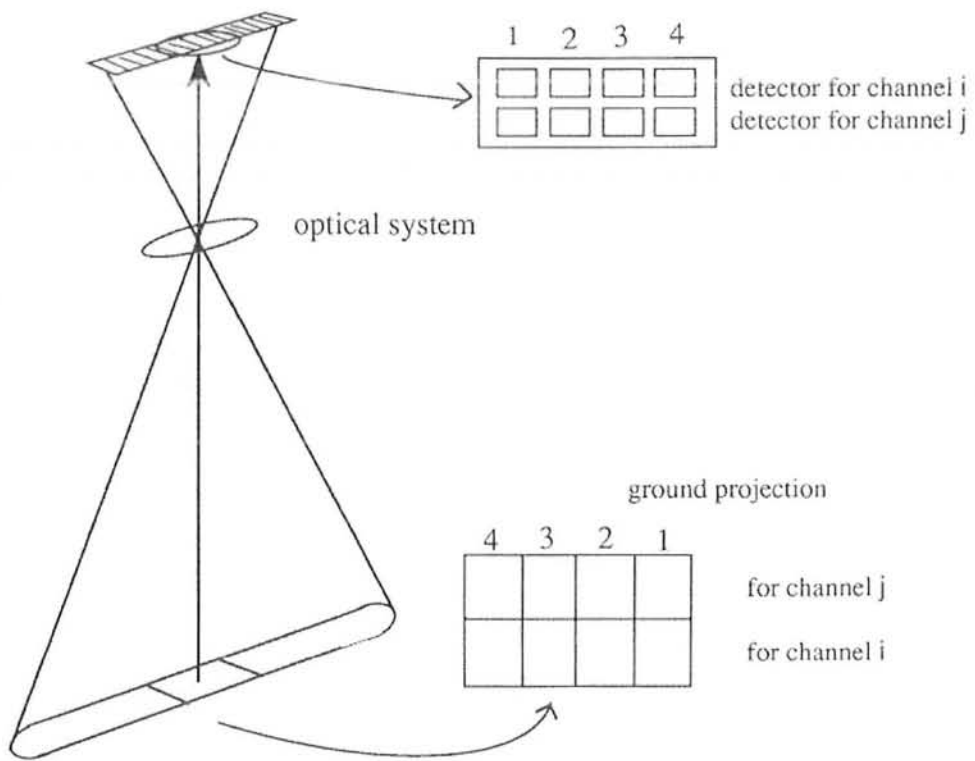**Figure2.3**: FOV and IFOV

Figure2.4: Relationship between detector and its ground projection

information in terms of bits is given by the following formula.

$$\log_2 n \text{ (bit)}$$

In remote sensing, the quantization level is normally 6, 8 or 10 bits. For computer processing, the unit of byte (1 byte = 8 bits integer value 0-255, 256 gray levels) is much more convenient. Therefore remote sensing data will be treated as one or two byte data.

The total data volume of multi-channel data per scene is computed as follows.

Data Volume (byte) = (line number) x (pixel number) x (channel number) x (bits) /8

Output data usually corresponds to the observed radiance detected by the sensor. The absolute radiance is converted by a linear formula from the observed radiance.

2.2 Format of Remote Sensing Image Data

Multi-band image data are represented by a combination of spatial position (pixel number and line number) and band.

The data format for multi-band images is classified into the following three type, as shown in Figure 2.5.

2.2.1 BSQ format (band sequential) image data (pixel number and line number) of each band are separately arranged.

2.2.2 BIL format (band interleaved by line) line data are arranged in the order of band number and repeated with respect to line number.

2.2.3 BIP format (band interleaved by pixel) A set of multi-band data with respect to each pixel arranged spatially by pixel number and line number.

For color image output, BSQ format would be convenient because three bands will be assigned to R(red), G(green) and B(blue). However BIP format would be better for classification by a maximum likelihood classifier because multi-band data are required pixel by pixel for the multi-variable processing. BIL would be a compromise between BSQ and BIP. Remote sensing data usually includes various annotation data in addition to image data. Since 1982, satellite image data have been provided in a standard format called World Standard Format, or LTWG format (specified by Landsat Technical Working Group). The World Standard Format has the data structure called super structure with three records of volume descriptor, file pointer and file descriptor which describe the contents of the data. Either BSQ or BIL format is chosen in the World Standard Format.
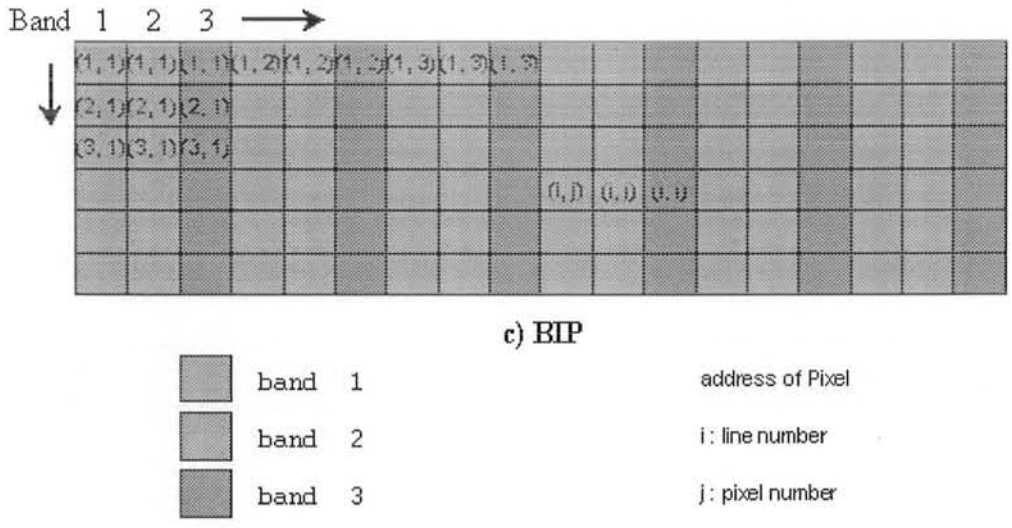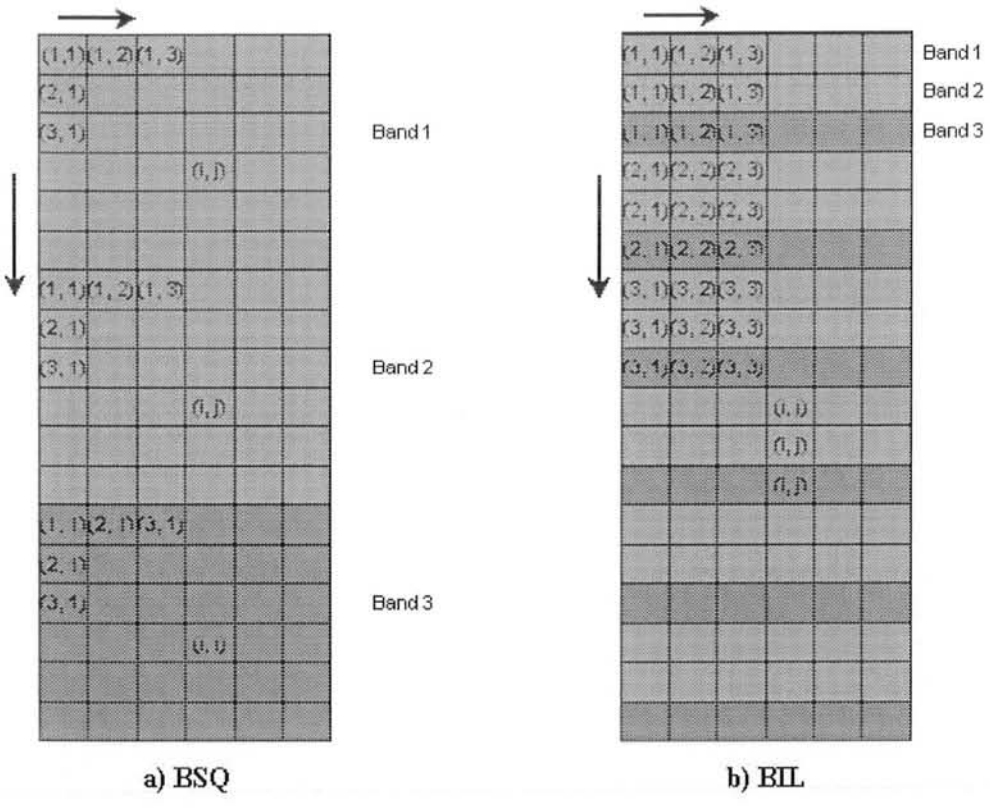
Figure2.5: Digital image data formats (in case of three separate bands)

2.3   Data Errors and Correction

As any image involves radiometric errors as well as geometric errors, these errors should be corrected. Radiometric correction is to avoid radiometric errors or distortions, while geometric correction is to remove geometric distortion.

- Radiometric Correction
- Geometric Correction

2.4   Radiometric Correction

When the emitted or reflected electro-magnetic energy is observed by a sensor on board an aircraft or spacecraft, the observed energy does not coincide with the energy emitted or reflected from the same object observed from a short distance. This is due to the sun's azimuth and elevation, atmospheric conditions such as fog or aerosols, sensor's response etc. which influence the observed energy. Therefore, in order to obtain the real irradiance or reflectance, those radiometric distortions must be corrected.

Radiometric correction is classified into the following three types

2.4.1   Radiometric Correction of Effects Due to Sensor Sensitivity

In the case of optical sensors, with the use of a lens, a fringe area in the corners will be darker as compared with the central area. This is called vignetting. Vignetting can be expressed by $\cos^n \theta$, where θ is the angle of a ray with respect to the optical axis. n is dependent on the lens characteristics, though n is usually taken as 4. In the case of electro-optical sensors, measured calibration data between irradiance and the sensor output signal, can be used for radiometric correction.

2.4.2   Radiometric Correction for Sun Angle and Topography

a. Sun Spot
The solar radiation will be reflected diffusely onto the ground surface, which results in lighter areas in an image. It is called a sun spot. The sun spot together with vignetting effects can be corrected by estimating a shading curve which is determined by Fourier analysis to extract a low frequency component

b.Shading
The shading effect due to topographic relief can be corrected using the angle between the solar radiation direction and the normal vector to the ground surface.

2.4.3   Atmospheric Effects

Various atmospheric effects cause absorption and scattering of the solar radiation. Reflected or emitted radiation from an object and path radiance (atmospheric scattering) should be corrected for.

2.4.4 Atmospheric Correction

The solar radiation is absorbed or scattered by the atmosphere during transmission to the ground surface, while the reflected or emitted radiation from the target is also absorbed or scattered by the atmosphere before it reaches a sensor. The ground surface receive not only the direct solar radiation but also sky light, or scattered radiation from the atmosphere. A sensor will receive not only the direct reflected or emitted radiation from a target, but also the scattered radiation from a target and the scattered radiation from the atmosphere, which is called path radiance. Atmospheric correction is used to remove these effects Figure 2.6. The atmospheric correction method is classified into the method using the radiative transfer equation, the method using ground truth data and other methods.

An approximate solution is usually determined for the radiative transfer equation. For atmospheric correction, aerosol density in the visible and near infrared region and water vapour density in the thermal infrared region should be estimated. Because these values cannot be determined from image data, a rigorous solution cannot be used.

At the time of data acquisition, those targets with known or measured reflectance will be identified in the image. Atmospheric correction can be made by comparison between the known value of the target and the image data (output signal). However the method can only be applied to the specific site with targets or a specific season.

A special sensor to measure aerosol density or water vapor density is utilized together with an imaging sensor for atmospheric correction. For example, the NOAA satellite has not only an imaging sensor of AVHRR (Advanced Very high Resolution Radiometer) but also HIRS (High Resolution Infrared Radiometer Sounder) for atmospheric correction.

2.5   Geometric Distortions of the Image

Geometric distortion is an error on an image, between the actual image coordinates and the ideal image coordinates which would be projected theoretically with an ideal sensor and under ideal conditions.

Geometric distortions are classified into internal distortion resulting from the geometry of the sensor, and external distortions resulting from the attitude of the sensor or the shape of the object.
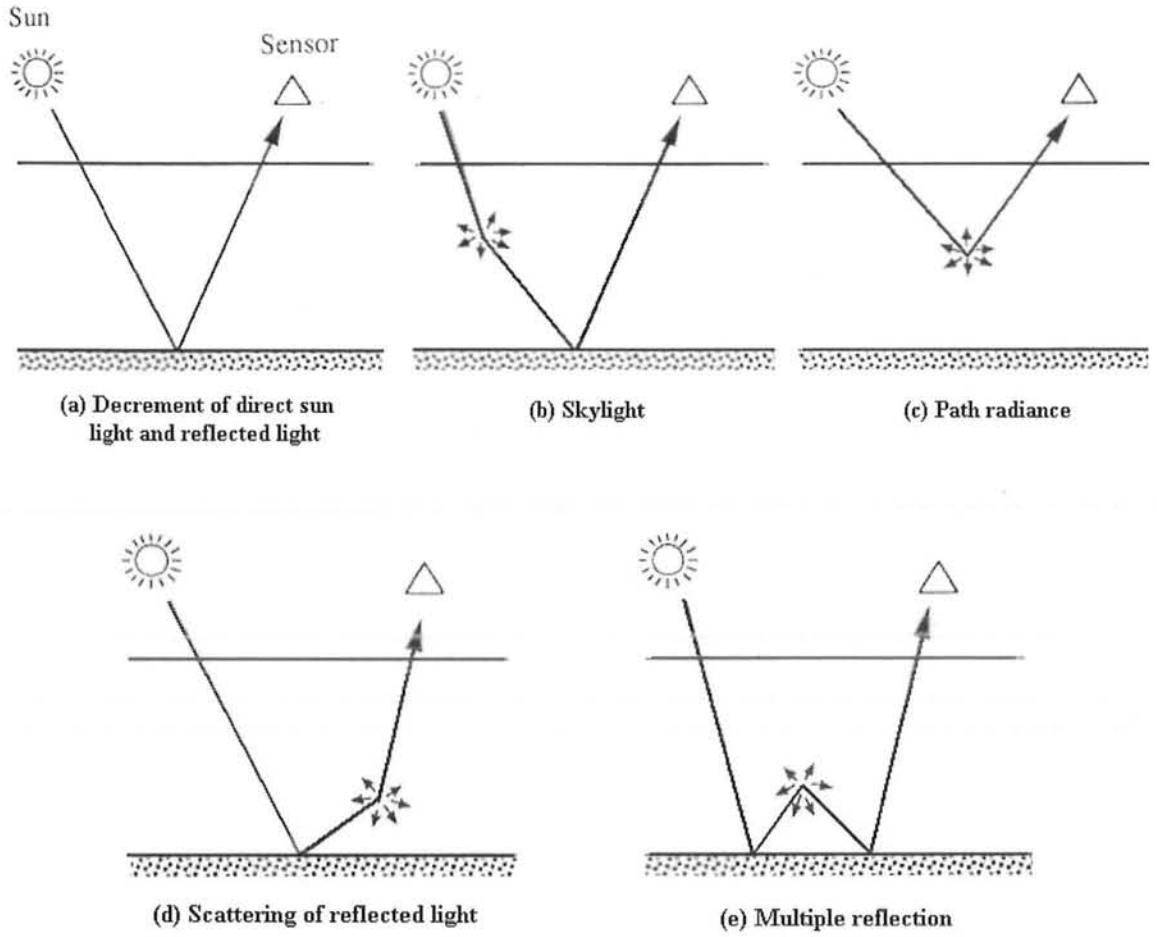
23

(a) Decrement of direct sun light and reflected light

(b) Skylight

(c) Path radiance

(d) Scattering of reflected light

(e) Multiple reflection

Figure2.6: Atmospheric effect

2.6   Geometric Correction

Geometric correction is undertaken to avoid geometric distortions from a distorted image, and is achieved by establishing the relationship between the image coordinate system and the geographic coordinate system using calibration data of the sensor, measured data of position and attitude, ground control points, atmospheric condition etc.

The steps to follow for geometric correction are as follows.

Selection of Method

After consideration of the characteristics of the geometric distortion as well as the available reference data, a proper method should be selected.

Determination of Parameters

Unknown parameters which define the mathematical equation between the image coordinate system and the geographic coordinate system should be determined with calibration data and/or ground control points.

Accuracy Check

Accuracy of the geometric correction should be checked and verified. If the accuracy does not meet the criteria, the method or the data used should be checked and corrected in order to avoid the errors.

Interpolation and Resampling

Geo-coded image should be produced by the technique of resampling and interpolation. There are three methods of geometric correction as mentioned below.

a. Systematic Correction

When the geometric reference data or the geometry of sensor are given or measured, the geometric distortion can be theoretically or systematically avoided. For example, the geometry of a lens camera is given by the collinearity equation with calibrated focal length, parameters of lens distortions, coordinates of fiducial marks etc. The tangent correction for an optical mechanical scanner is a type of system correction. Generally systematic correction is sufficient to remove all errors.

b. Non-Systematic Correction

Polynomials to transform from a geographic coordinate system to an image coordinate system, or vice versa, will be determined with given coordinates of ground control points using the least square method. The accuracy depends on the order of the polynomials, and the number and distribution of ground control points.

c. Combined Method

Firstly the systematic correction is applied, then the residual errors will be reduced using lower order polynomials. Usually the goal of geometric correction is to obtain an error within plus or minus one pixel of its true position.

2.7   Image Enhancement and Feature Extraction

Image enhancement can be defined as conversion of the image quality to a better and more understandable level for feature extraction or image interpretation, while radiometric correction is to reconstruct the physically calibrated value from the observed data.

On the other hand, feature extraction can be defined as the operation to quantify the image quality through various parameters or functions, which are applied to the original image.

These processes can be considered as conversion of the image data. Image enhancement is applied mainly for image interpretation in the form of an image output, while feature extraction is normally used for automated classification or analysis in a quantitative form.

Typical image enhancement techniques include gray scale conversion, histogram conversion, color composition, color conversion between RGB and HSI, etc., which are usually applied to the image output for image interpretation.

Features involved in an image are classified as follows.
(1) Spectral features
special color or tone, gradient, spectral parameter etc.
(2) Geometric features
edge, linearment, shape, size, etc.
(3) Textural features
pattern, spatial frequency, homogeneity, etc.

2.8   Operations Between Images

Operations between multi-spectral images or multi-date images are very useful for image enhancement and feature extraction.

Operations between images include two techniques; arithmetic operation and logical operation.

2.8.1 Arithmetic Operations

Addition, subtraction, multiplication, division and their combinations, can be applied for many purposes, including noise elimination. As the results of the operation can sometimes negative or small values between 0 and 1, they should be adjusted to a range, usually in eight bits or 0 to 255 for image display.

Typical operations are ratioing, for geological feature extraction, and normalized difference vegetation index, for vegetation monitoring with NOAA AVHRR data or other visible near infrared sensors.

2.8.2 Ratioing

Ratio = X_i / X_j

Ratioing may be useful for geological feature extraction. Such ratioing can be applied to multi-temporal thermal infrared data for extraction of thermal inertia.

2.8.2 Normalized Difference Vegetation Index(NDVI)

$$NDVI = ch.2 - ch.1 \div ch.2 + ch.1$$

where ch.1 : red band
ch.2 : infrared band

NDVI shows as a high value for denser vegetation, while the NDVI is very low in desert, or non-vegetation regions.

2.8.3 Logical Operation
Logical addition (OR set), logical multiplication (AND set), true and false operations etc. can be applied to multi-date images or a combination of remote sensing images and thematic map images.

For example a remote sensing image or the classified result can be overlaid on map data, such as political boundaries. Such an overlay will be very useful for change detection.

2.9   Spatial Filtering

Spatial filtering is used to obtain enhanced images or improved images by applying, filter function or filter operators in the domain of the image space (x,y) or spatial frequency (x,h). Spatial filtering in the domain of image space aims at image

SPATIAL FILTERS	3 × 3 OPERATOR	EFFECTS
Sobel	$\lvert A \rvert + \lvert B \rvert$ or $\sqrt{A^2+B^2}$ where, $A=\begin{bmatrix} -1 & 0 & -1 \\ -2 & 0 & 2 \\ -1 & 0 & 1 \end{bmatrix}$ $B=\begin{bmatrix} -1 & -2 & -1 \\ 0 & 0 & 0 \\ 1 & 2 & 1 \end{bmatrix}$	gradient (finite differences)
Prencit	$\lvert A \rvert + \lvert B \rvert$ or $\sqrt{A^2+B^2}$ where, $A=\begin{bmatrix} -1 & 0 & 1 \\ -1 & 0 & 1 \\ -1 & 0 & 1 \end{bmatrix}$ $B=\begin{bmatrix} -1 & -1 & -1 \\ 0 & 0 & 0 \\ 1 & 1 & 1 \end{bmatrix}$	gradient (finite differences)
Laplacian	$\begin{bmatrix} 0 & -1 & 0 \\ -1 & 4 & -1 \\ 0 & -1 & 0 \end{bmatrix}$ or $\begin{bmatrix} -1 & -1 & -1 \\ -1 & 8 & -1 \\ -1 & -1 & -1 \end{bmatrix}$	differential
smoothing	$\begin{bmatrix} 1/9 & 1/9 & 1/9 \\ 1/9 & 1/9 & 1/9 \\ 1/9 & 1/9 & 1/9 \end{bmatrix}$ or $\begin{bmatrix} 0 & 1/5 & 0 \\ 1/5 & 1/5 & 1/5 \\ 0 & 1/5 & 0 \end{bmatrix}$	
median	Replaced with median of 3 × 3 window	smoothed image
high-pass	$\begin{bmatrix} 0 & -1 & 0 \\ -1 & 5 & -1 \\ 0 & -1 & 0 \end{bmatrix}$ or $\begin{bmatrix} -1/9 & -1/9 & -1/9 \\ -1/9 & 8/9 & -1/9 \\ -1/9 & -1/9 & -1/9 \end{bmatrix}$	edge-enhancement
sharpening	$\begin{bmatrix} 1/9 & -8/9 & 1/9 \\ -8/9 & 37/9 & -8/9 \\ 1/9 & -8/9 & 1/9 \end{bmatrix}$	clear image

Table1: Examples of some spatial filters

enhancement with so-called enhancement filters, while in the domain of spatial frequency it aims at reconstruction with so-called reconstruction filters.

2.9.1 Filtering in the Domain of Image Space

In the case of digital image data, spatial filtering in the domain of image space is usually achieved by local convolution with an n x n matrix operator.

The convolution is created by a series of shift-multiply-sum operators with an n x n matrix (n: odd number). Because the image data are large, n is usually selected as 3, although n is sometimes selected as 5, 7, 9 or 11.

Table1 shows typical 3 x 3 enhancement filters.

2.9.2 Filtering in the Domain of Spatial Frequency

Filtering in the domain of spatial filtering uses the Fourier transformation to convert from image space domain to spatial frequency domain as follows.

$G(u,v) = F(u,v) H(u,v)$

F: Fourier transformation of input image
H: filter function

An output image from filtering of spatial frequency, can be obtained by using an inverse Fourier transformation of the above formula.

Low pass filters, high pass filters, band pass filters etc., are typical filters with a criterion of frequency control. Low pass filters which out puts only lower frequency image data, less than a specified threshold, can be applied to remove high frequency, noise,while high pass filter are used for removing, for example, stripe noise of low frequency.

2.10 Classification Techniques

Classification of remotely sensed data is used to assign corresponding levels with respect to groups with homogeneous characteristics, with the aim of discriminating multiple objects from each other within the image.

The level is called class. Classification will be executed on the base of spectral or spectrally defined features, such as density, texture etc. in the feature space. It can be said that classification divides the feature space into several classes based on a decision rule. Figure 2.7 shows the concept of classification of remotely sensed data
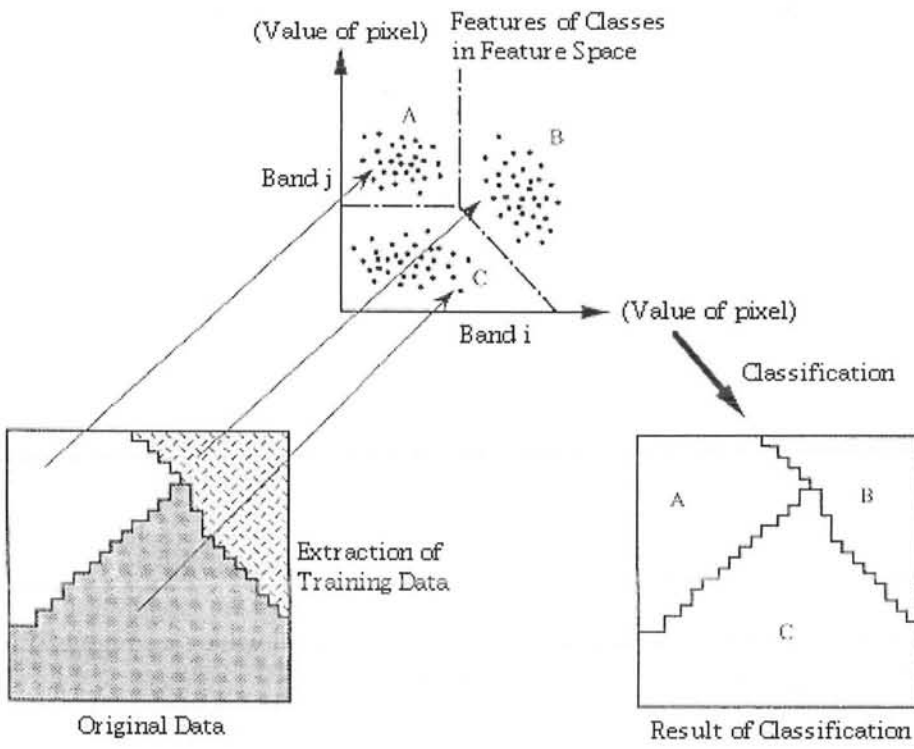
Figure2.7: Concept of Classification of Remotely Sensed Data

In many cases, classification will be undertaken using a computer, with the use of mathematical classification techniques. Classification will be made according to the following procedures.

Step 1: Definition of Classification Classes

Depending on the objective and the characteristics of the image data, the classification classes should be clearly defined.

Step 2: Selection of Features

Features to discriminate between the classes should be established using multi-spectral and/or multi-temporal characteristics, textures etc.

Step 3: Sampling of Training Data

Training data should be sampled in order to determine appropriate decision rules. Classification techniques such as supervised or unsupervised learning will then be selected on the basis of the training data sets.

Step 4: Estimation of Universal Statistics

Various classification techniques will be compared with the training data, so that an appropriate decision rule is selected for subsequent classification.

Step 5: Classification

Depending up on the decision rule, all pixels are classified in a single class. There are two methods of pixel by pixel classification and per-field classification, with respect to segmented areas.

Popular techniques are as follows.
a. Multi-level slice classifier
b. Minimum distance classifier
c. Maximum likelihood classifier
d. Other classifiers such as fuzzy set theory and expert systems

Step 6: Verification of Results

The classified results should be checked and verified for their accuracy and reliability.

2.11   DEM and DTM

A DEM (digital elevation model) is digital representation of topographic surface with the elevation or ground height above any geodetic datum. Figure 2.8 shows three major DEMs that are widely used GIS.

A DTM (digital terrain model) is digital representation of terrain features including elevation, slope, aspect, drainage and other terrain attributes. Usually a DTM is derived from a DEM or elevation data. In this book, a DEM refers to a model with elevation data in digital format by which elevation at an arbitrary location in the area can be interpolated, while a DTM refers to terrain features in digital format, that can be derived from the elevation data.

Figure 2.9 shows several terrain features including the following DTMs.

- Slope and Aspect
- Drainage network
- Catchment area
- Shading
- Shadow
- Slope stability

2.11.1 Generation of Contour Lines

Contour lines are one of the terrain features, which represent the relief of the terrain with the same height.

There are two types of contour lines in visualizing GIS data; vector line drawing and raster image.

2.11.2 Vector Line Drawing

In case when the terrain points are given in grid, the simplest method is to divide the square cell into two triangles mechanically. However such mechanical division will cause some inconveniences in smoothness of the contour lines.

In case when the terrain points are given randomly, TINs will be created.

2.11.3 Raster Image

Contour image with painted contour terraces, belts or lines instead of vector lines will be generated in raster form.

In case of grid, highly densed subgrid points will be generated and the interpolated height values, which are simply sliced into contour interval, are assigned to the corresponding

(a) Grid Cell DEM   (b) TIN   (c) Contour Lines
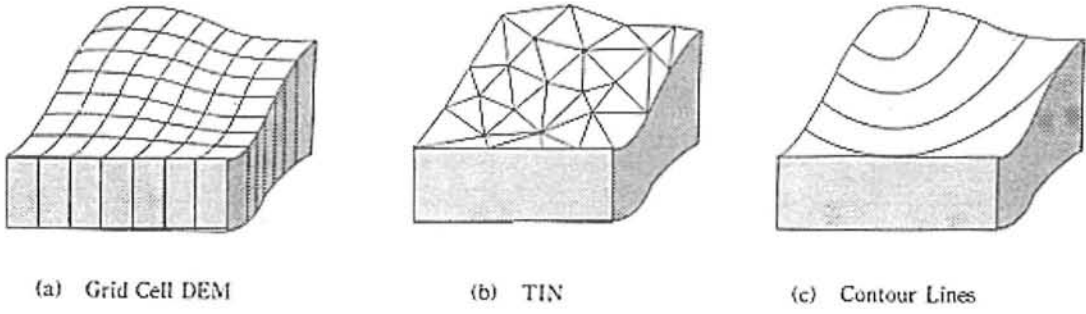
Figure2.8: Types of DEMs, widely used in GIS

(a) Slope and Aspect   (b) Drainage Network   (c) Catchment Area

(d) Shading   (e) Shadow   (f) Slope Stability
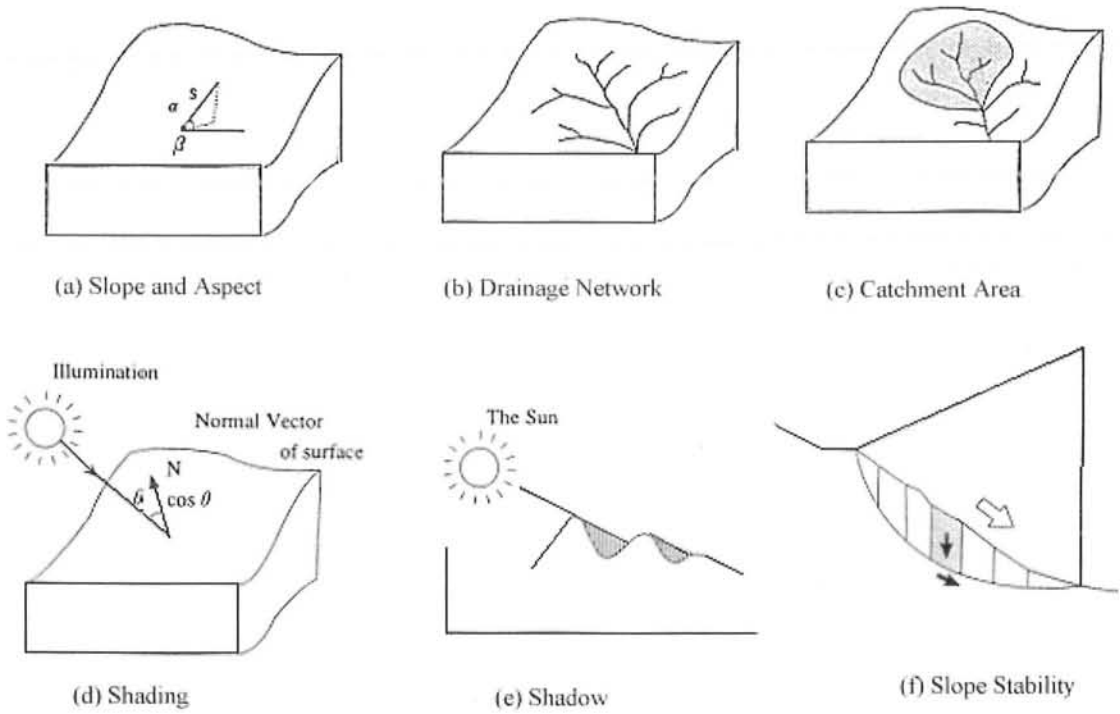
Figure2.9: Terrain features including the DTMs

color. In case of irregularly spaced points, two-step interpolation that is coarse grid and then dense subgrid will be applied. The procedure is known as densification.

2.12   Interpolation of Elevation from Contours

Digital elevation model (DEM) is very often generated by measuring terrain points along contour lines using a digitizer. DEM with contour points should be provided with an algorithm interpolate elevation at arbitrary points.

There are several interpolation methods as follows.

2.12.1 Profile Method

A profile passing through the point to be interpolated will be generated and linear or spline curve applied. However, sometimes improper profiles are introduced. In case of spline curve, transition areas from steep to gentle slope will be a problem of wave shape profile.

2.12.2 Proportional Distance Method

According to distance to two adjacent contour lines, the elevation is interpolated proportionally with respect to the distance ratio. However a point in an island contour, would be a problem.

2.12.3 Window Method

A circular window is set up around a point to be interpolated and adjacent terrain points are used to interpolate the value using second order or third order polynomials.

The interpolation accuracy is better than other methods, but searching of adjacent points within the window is time consuming.

2.12.4 TIN Method

TINs are generated using terrain points along contour lines. The interpolation is very easy but TINs within an island, would be a problem.

Buffering based on proportional method with additional independent terrain points will be the best interpolation method.

2.13   GIS and Remote Sensing

For the users of remote sensing, it is not sufficient to display only the results obtained from image processing. For example, to detect land cover change in an area is not enough, because the final goal would be to analyze the cause of change or to evaluate the impact of change. Therefore the result should be overlaid on maps of transportation

facilities and land use zoning. In addition, the classification of remote sensing imagery will become more accurate if the auxiliary data contained in maps are combined with the image data.

In order to promote the integration of remote sensing and geographic data, geographic information system (GIS) should be established in which both the image and graphic data are stored in a digital form, retrieved conditionally, overlaid on each other and evaluated with the use of a model.

The following three functions are very important in GIS.

(1) To store and manage geographic information comprehensively and effectively

(2) To display geographic information depending on the purpose of use

(3) To execute query, analysis and evaluation of geographic information effectively

2.14 Model and Data Structure

In order to process and manage geographic information by computers, it is necessary to describe the spatial location and distribution, as well as the attributes and characteristics, according to a specified form, termed a spatial representation model with a standardized data structure.

Geographic information can be represented with geometric information such as location, shape and distribution, and attribute information such as characteristics and nature.

Vector and raster forms are the major representation models for geometric information.

2.14.1 Vector Form and its Data Structure

Most objects on a map can be represented as a combination of a point (or node), edge (or arc) and area (or polygon). The vector form is provided by the above geometric factors. The attributes are assigned to points, edges and areas.

The data structure is specified for the vector form as follows.

A point is represented by geographic coordinates. An edge is represented by a series of line segments with a start point and an end point. A polygon is defined as the sequential edges of a boundary. The inter-relationship between points, edges and areas is called a topological relationship. Any change in a point, edge or area will influence other factors through the topological relationship. Therefore the data structure should be specified to fulfill the relationship.

2.14.2 Raster Form and its Data Structure

In the raster form, the object space is divided into a group of regularly spaced grids (sometimes called pixels) to which the attributes are assigned. The raster form is basically identical to the data format of remote sensing data.

As the grids are generated regularly, the coordinates correspond to the pixel number and line number, which is usually represented in a matrix form.

2.15 Spatial Analysis

Spatial analysis is used to produce additional geographic information using existing information or to enhance the spatial structure or relationship between geographic information. Many techniques have been proposed, as follows.

The following three techniques are very often used in GIS.

2.15.1 Overlay Technique

Various geographic data comprised of multiple layers are overlaid with logical operations including logical addition or logical multiplication. For example, a hazard risk area of soil erosion can be estimated by overlaying deforested and slope gradient maps in a mountainous area.

2.15.2 Buffering Technique

Buffering is to find an area the within a certain distance from a given point or a line. For example noise polluted areas will be extracted by buffering an area within 30 meter distance from a trunk road.

2.15.3 Volonoi Tessellation

An area may be divided in a group of "influential areas" termed Volonoi tessellation, that can be formed by bisectors between spatially distributed points. For example, a school zone can be drawn by Volonoi tessellation between differently located schools.

Spatial auto-correlation is one of the statistical techniques to find the spatial structure of geographic information. Spatial auto-correlation is a correlation factor between two differently located events. High accuracy spatial interpolation can be executed with a lower density of samples in the case of high spatial auto-correlation.
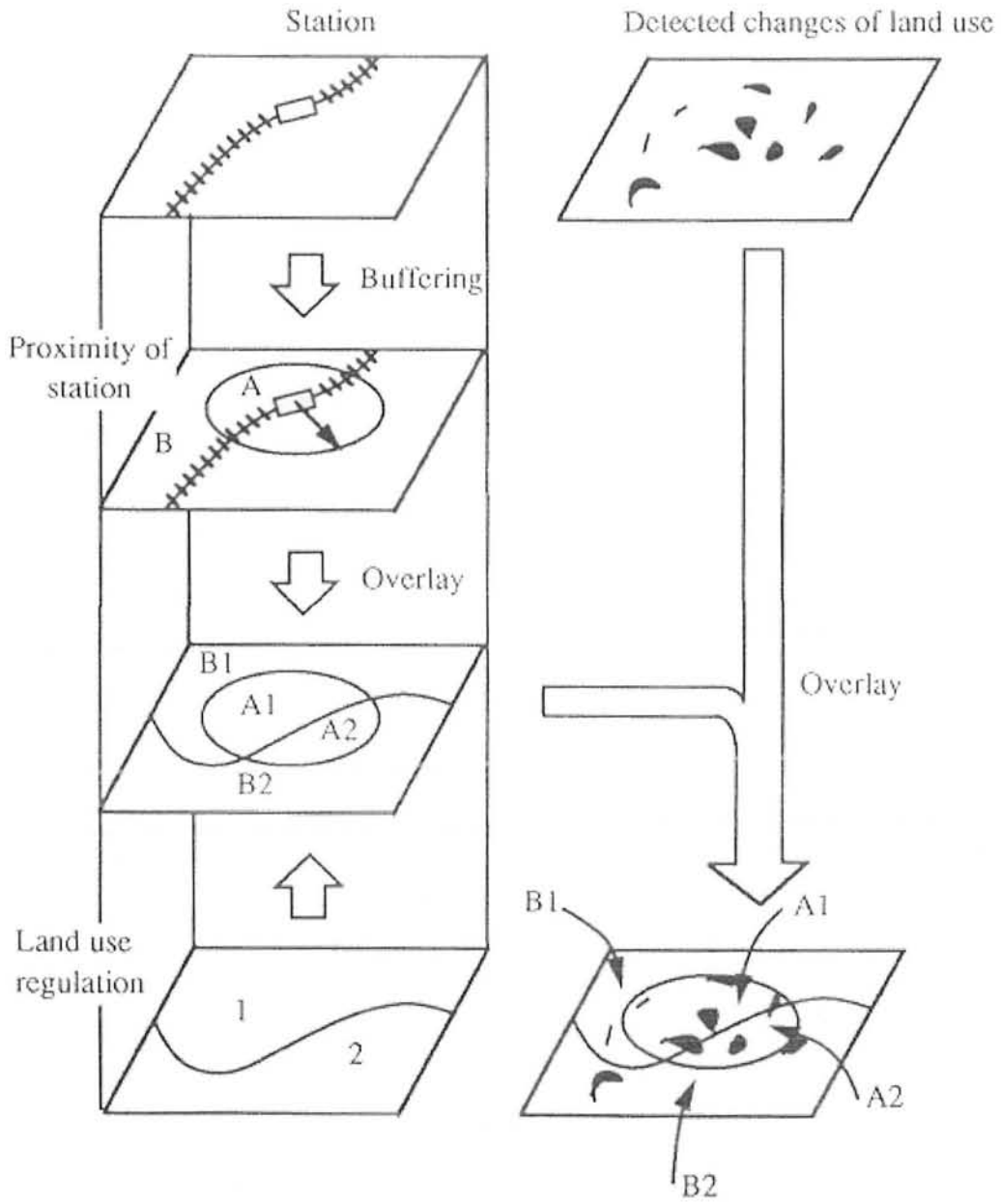
Figure2.10: A combined technique using remote sensing, buffering and overlay

Figure 2.10 shows an example of a combined technique using remote sensing, buffering and overlay. In this example, the land use change ratio is tabulated with respect to accessibility to a railway station and land use zoning.

2.16   Use of Remote Sensing Data in GIS

Remote sensing data after geometric correction, can be overlaid on other geographic data in a raster form. In GIS, there are two uses of use of remote sensing data; as classified data and as image data.

Land cover maps or vegetation maps classified from remote sensing data can be overlaid onto other geographic data, which enables analysis for environmental monitoring and its change.

Remote sensing data will be classified or analyzed with other geographic data to obtain a higher accuracy of classification. Image data are sometimes also used as image maps, with an overlay of political boundaries, roads, railways etc. Such an image map can be successfully used for visual interpretation.

If a digital elevation model (DEM) is used with remote sensing data, shading corrections in mountainous areas can be made by dividing by cos q (where q : angle between sun light and the normal to the sloping surface).

Chapter 3

CASE STUDY

3.1 Introduction

Spreading water scarcity is one of the most important issues that the world is facing today. By now many of us have read dastardly predictions about water being the major cause of the wars in the near future as well as creating a new breed of refugees, the 'water refugees.

What has caused the alarm bells to ring is the fact that water use globally has increased three-fold during the last fifty years. The tremendous increase in water consumption globally has also resulted in massive underground pumping which still continues to rise. The massive water pumping in turn has resulted in falling of water tables on every continent including the Indo-Pakistan subcontinent.

As 70 per cent of all the water pumped from underground or drawn from rivers is used for irrigation, water scarcity also means food scarcity. That explains the rising grain imports in many countries including India, Iran, Mexico, Egypt, China and Pakistan, an agro-based economy. The case of Saudi Arabia is only slightly different, the country, which turned to wholesale use of pumped water for agriculture in the 1970s, had to import 7 million tonnes of grain in 1997 compared to 3 million tonnes three years ago when its aquifers began to dry up in 1994.

The history of dam construction in Pakistan is rather short. The perennial rivers served the irrigation need. Pakistan has hydropower potential of 33,000 MW, of which only 15% has been exploited. The 1st major hydropower project built in 1960 was warsak dam. Mangla and Tarbela dams in addition to creating storages provide the much-needed hydropower.

Mangla Dam Project was actually conceived in 1950's as a multipurpose project to be constructed at a place called Mangla on river Jehlum located about 30 km upstream of Jehlum city (120 km from Capital Islamabad). The initial investigation and its feasibility studies were completed in 1958. Later on the project was included in the Indus Basin Project. The construction of Mangla Dam was started in 1962 and completed in 1967. Mangla Dam is a multipurpose project primarily meant for affecting part replacement of water supplies of three eastern rivers from Jehlum river. Besides, it is designed to conserve and control flood water of river Jehlum through significant reduction in flood peaks and volumes at downstream by incidental use of the available storage space. The other by products are power generation to meet the power demand of the country, fish culture to provide protein rich diet, tourism to provide healthy recreation facilities to the people. The project consists of two dams (Main Dam & Jari Dam), two dykes to contain reservoir, two spillway for outflow regulations, intake structures with five tunnels, a power house and a tailrace canal.

Statistics of Mangla Dam

Type	Earth-fill	
Max. Height (above core trench)	454 ft.	138.38 meters
Max. Height (above river bed)	380 ft.	115.57 meters
Crest Elevation	1234 ft.	376.12 meters
Length of Crest	11000 ft.	3353 meters
Max. Conservation Level	1202 ft.	366.37 meters
Min Operation Level	1040 ft.	317.0 meters
Design Gross Storage	5.88 MAF	
Existing Gross Storage	4.823 MAF	

3.2   Objectives:

This particular study has been attempted to exploit the potential of SRS data for;

1)-   Monitoring Temporal Changes.
2)-   Monitoring of Dam Siltation.
3)-   Movement of sediments.
4)-   To calculate the increase in the storage capacity of dam.
5)-   How much area (residential, agriculture & forests) will be affected by this increased amount of water.

3.3   Risks Faced by Mangla Dam

There will be a loss of capacity in existing reservoirs by 2.91 MAF(Million Acer Feet) upto the year 2000, and that 3.6 MAF storage is required for assuring the water availability to provinces under the Water Accord, 1991. As far as the life of the reservoir is concerned, it was envisaged to 125 years for Mangla in the original projects, which has been revised to 225 years due to lower rate of siltation than estimated. The rate of siltation will be further reduced as WAPDA has already initiated a large scale watershed management programme in the catchment areas of the reservoir, though they have not published the results achieved. WAPDA had made a study of siltation of reservoirs in 1988, in which, extent of siltation of the reservoirs was indicated to be 1.23 MAF and the annual rate of siltation of live storage was indicated to be 0.081 MAF for all three reservoirs. Adopting WAPDA's figure of 0.081 MAF of siltation per year, further loss of capacity has occured about 1 MAF more in the 12-13 years from 1988 upto the year 2000[6].

3.3.1 Sedimentation and its Sources

The Jehlum River has its source in the Himalayan catchment area and emerges from the land of glaciers on the Northern slopes of the Kashmir, it largely brings in snowmelt supplies in addition to some monsoon rains. Main upstream tributaries join the Jehlum are Neelum, Poonch and Kunhar rivers.

At Mangla, the Jehlum River drains a catchment area of 33,334 km^2 [5] mostly comprising a glaciated landscape. Most of the catchment area is located in a monsoon environment. The Jehlum is, in fact, one of the larger sediment producing rivers of the world.

The main source of inflow of sediment is glacial and snowmelt. The glacial flow and snowmelt is also an indicator that plantations beyond the snowline are not possible. It is not possible, therefore, to control the geologic erosion. Furthermore, glacial and snowmelt is drained to the river through steep slopes in formations which are geologically young.

Because the sediment inflow to Mangla reservoir was known to be very high, during the design phase, investigated the feasibility during the high run-off season principally in June and July when over 50 % of the annual sediment load occurred.

3.4 Study Area

Mangla Dam is located about 80 Km southeast of Islamabad at the border of Pakistan and Azad Jammu & Kashmir. It is situated at $32^0.5'$ North latitude and $73^0.7'$ longitudes East. It is on river Jehlum. The Mangla reservoir has been designed and constructed for gross storage capacity of 5.88 MAF at the normal conservation level of 1202 ft. above sea level. The reservoir can be drawn down to 1040 ft. above sea level thus leaving a dead storage of 0.54 MAF.It is 1234 feet high above sea level. It is 2nd largest dam of the country with generating capacity of 1800 mega watts. Every year a large amount of

Catchment [Area, sq. km.] *(% of Mangla Dam catchment)*	Annual Potential Water contribution	
	Million Acre Feet	**%**
Jhelum River [19, 321], *(58%)*	19.935	58
Neelum River [7,356], *(22%)*	5.110	16
Punch River [4,222], *(13%)*	3.632	12
Kunhar River [2,435], *(7%)*	2.470	8
MANGLA DAM [33,334], *(100%)*	31.147	100

sediments are deposited in reservoir due to which its storage capacity is decreasing gradually.

The total catchment of Mangla Dam is spread over an area of about 33,334 sq.km. Mangla Lake is fed by Jehlum, Neelum, Punch, Kunhar rivers and their tributaries. The catchment areas of above rivers, their relative percentages with reference to total Mangla Dam catchment area and potential annual water contribution from each are shown in Table[5]. A range of 1000 – 2000 mm rain is averaged out to 1250 mm for a period of full year; similarly 500 – 1000 mm to 625 mm and that mentioned to be receiving rain above 2000 mm in the FEP Atlas [10] was taken as 2250 mm for the sake of computation of the potential volume of water which could flow into Mangla Lake annually. The estimated potential water contribution and relative catchment areas of different rivers are graphically compared in Table [5].

Literature Survey

Some literature has reviewed for the previous siltation effects on Mangla dam and its causes some of the important features about Mangla dam which were discussed in literature are summarized here [6].

3.5   Predicted and Actual Sedimentation Rates

The first assessment of the rate of Sedimentation in the Mangla reservoir was made by the Project Consultant on the basis of the limited sediment sampling data obtained by the Punjab Irrigation Research Institute, Lahore during the period from 1954 to 1957, assuming the bed load to be 15 percent of the suspended load, sediment density of 81 lb. per cu. ft. and the reservoir trap efficiency of 90 percent, the Consultants estimated the average rate of sedimentation to be 40,000 AF(Acer Feet) per year. On this basis, it was assumed that the life of the Mangla reservoir would be of the order of 125 years.

On the basis of the observations made from year 1960 onward, the revised estimate of the average annual rate of Sedimentation was found to be 61000 AF with bed load assumed at 10 percent of the suspended sediment and ultimate sediment density of 83.6 lb. per cu. ft.

The 1969 study also indicates that although Jehlum Branch of Mangla Reservoir would take 70 years before it is completely silted up (except 0.5 MAF with in the influence zone of the Reservoir releases), the delta fronts and the sediment advancing in the Jehlum River Branch would take about 40 years to reach the Kanshi River confluence and would require another five years to extend the delta fronts to the confluence with the Poonch River resulting formation of barriers, which would trap about 2.6 MAF of useful storage in the Poonch and Kanshi Branches. As the life of Kanshi and Poonch pocket of the reservoir were estimated to be 175 and 200 years respectively, it is obvious that a successful programme of reducing the sediment inflow from the Jehlum catchment would not only prolong the life of Jehlum Branch but would delay the formation of the delta at its confluence with Kanshi and Poonch pockets, thus conserving a substantial trapped

water storage of 2.6 MAF in the two cropped up even after the super flood of 1992 as was anticipated.

As the estimates of Sediment inflows into Mangla Reservoir were based on suspended sediments sampling, it is obvious that these estimates were more or less theoretical compared to the actual measurements of sediment deposits in reservoir by hydrographic survey during the last 34 years or they have under estimated the outflow of sediments through Power Station/Spillway.

3.6   Causes of Sedimentation in Mangla Reservoir

The 12870 sq. miles catchment area of rivers Jehlum, Poonch, Khad and Kanshi above Mangla being mountainous is subjected to weathering under the severe climatic condition. Cutting of trees, urban developments in the area, and heavy rainfall are the major causes of movement of the sediments in the rivers. The velocity of the inflows containing sediments decreases upon entering Mangla Reservoir, which reduces the sediment carrying capacity of river water. The course sediments tend to deposit in the upper reaches of the reservoir, while the finer particles travel downstream towards the Dam and settle in reservoir.

3.7   Gross Storage Capacity

Gross storage capacity of the reservoir has been reduced from 5.88 MAF to 4.76 MAF as per 2000 hydrographic survey, conducted by WAPDA, with average annual sediment load of 33000 AF. The reservoir is loosing its capacity at a rate of 0.6% annually. Analysis of data shows that sediment was brought more during the years when high floods occurred. Incoming sediment as per third (1973 to 1978) and the sixth (1988 to 1992) hydrographic surveys was about 80% higher than the sediment deposited as per remaining 6% hydrographic surveys. This was due to major floods that occurred in the years 1976, 1978 and 1992.

3.7.1   Distribution of Sediment in the Dead Storage Zone

Original dead storage capacity of the reservoir has reduced from 0.54 MAF to 0.14 MAF. About 74% of dead storage capacity have been exhausted. Rate of loss in dead storage is increasing with the passage of time. From 1967 to 1988 sediment deposited in the dead storage zone was 0.19 MAF where in 10 years from 1987 to 2000, the sediment deposited in this zone was 0.21 MAF. The sharp depletion of reservoir in dead storage zone is mainly due to the following reasons.

- Flood of 1992 brought sediment more than the annual average sediment and deposited in the dead storage zone.

- Lowering the reservoir close to minimum operating level and longer stay due to low flows in Rabi and early Kharif seasons in the years 1994 and 1997 caused erosion of reservoir bed upstream of the delta pivot line and pushing sediment into the dead storage.

3.7.2   Distribution of Sediment in Live Storage Zone

Live storage capacity of the reservoir has reduced from 5.34 to 4.62 MAF Sediment deposited in this zone is 0.73 MAF and loss of live storage is about 15%. About 80% of live storage sediment have deposited in the lower reaches of the reservoir from El. 1040 ft to 1120 ft. The remaining 20% sediment falls in the upper reaches from El. 1120 ft to 1202 ft. Distribution of sediment shows that there is less sediment deposition in the upper reaches of the reservoir from El. 1180 ft to 1202 ft.

3.8   Reservoir Pockets

The reservoir consists of six pockets namely Jehlum Upper, Jehlum Lower, Kanshi, Pooch, Main and Khad & Jari Pockets as shown in Figure3.1. Original and remaining

45

capacity of various pockets is shown in Figure 3.1. Detail of each pocket is discussed as under:-

3.8.1 Jehlum Upper Pocket

This pocket lies in upper reach of reservoir and Jehlum River directly enters into this pocket. Original capacity of the pocket was 0.61 MAF and the remaining capacity of the pocket is 0.36 MAF. About 41% capacity of the pocket has been encroached by sediments. Rate of sediment deposition was higher during initial years of operation of the project and it gradually decreased. The latest survey shows that there is a slight increase of capacity by 1000 AF due to erosion in upper reaches of the pocket.

3.8.2 Jehlum Lower Pocket

Original capacity of this pocket was 0.36 MAF and 42% capacity of this pocket has been reduced due to sedimentation. The remaining capacity of the pocket is 0.21 MAF. The latest hydrographic survey indicates that the capacity of the pocket increased slightly due to erosion in the pocket.

3.8.3 Kanshi Pocket

This is smallest pocket of the reservoir having gross storage capacity 0.28 MAF. 21% of capacity has been reduced due to sedimentation and the remaining capacity is 0.22 MAF. The latest survey shows that rate of deposition of sediment has decreased in this pocket. Kanshi pocket joins the Jehlum lower pocket.

3.8.4 Poonch Pocket

Poonch River enters in this pocket. Original capacity of this pocket was 1.28 MAF. The remaining capacity is 1.05 MAF and 18% of it has been encroached by sediments. Results of previous all hydrographic surveys indicate that rate of deposition of sediment remained stable.
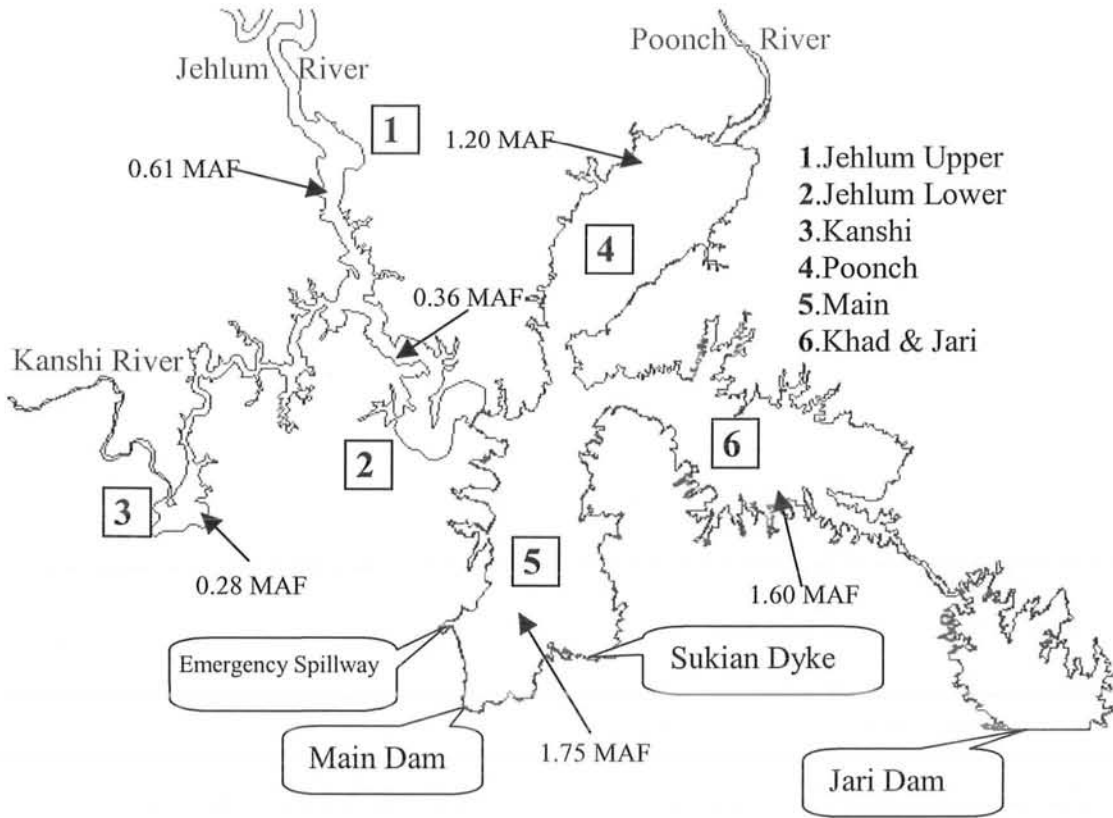
46

Jehlum River

Poonch River

1.20 MAF

0.61 MAF

1. Jehlum Upper
2. Jehlum Lower
3. Kanshi
4. Poonch
5. Main
6. Khad & Jari

0.36 MAF

Kanshi River

0.28 MAF

Emergency Spillway

1.60 MAF

Sukian Dyke

Main Dam

1.75 MAF

Jari Dam

Figure3.1: General Plan of Mangla Dam Sketched on Vector Layer
of Reservoir Boundary for 2002

3.8.5 Main Pocket

This is the biggest pocket of the reservoir with original storage capacity of 1.75 MAF. Jehlum Lower and Poonch pockets join this pocket. Rate of deposition of sediment in this pocket has increased with passage of time. About 56000 AF sediment was deposited from the year 1967 to 1988 in twenty years whereas 2,46,400 AF sediment was deposited from 1988 to 2000. Remaining capacity of this pocket is 1.43 MAF and storage loss is about 18%. This is the most affected part of the resevoir.

3.8.6 Khad and Jari Pocket

This pocket is adjacent to the main pocket. Jari pocket is separated from main pocket at El. 1102 ft. Erosion at junction of both the pockets is lowering the separation level with passage of time. No river directly enters in this pocket. Therefore rate of sedimentation is lower than the other pockets and 8% of capacity has been reduced so far. Original and present capacities are 1.60 and 1.48 MAF respectively. Rate of sediment deposition has decreased with the passage of time. The latest hydrographic survey shows no change in the capacity of this pocket.

3.9 Delta Profile

The major delta is advancing toward the dam and at present its pivot point is at approx, 5 miles upstream of the Main Dam as shown in fig. The delta pivot point is at El. 1054.9, which is 15 ft above the dead storage level. The depths of sediment deposited at the pivot point and in front of intake structures are 149 ft and 59 ft respectively. Slope of the fore set of major delta is 25 ft/mile while that of the bottom set is about 4 ft/mile. Results of the previous hydrographic surveys indicate that delta is advancing, pivot point is rising and fore set slope is steepening. Bed levels in front of intake structure are gradually rising whereas this survey indicates that pivot point retreat slightly as compared to 1997 survey.

3.10 Remedial Options

To reduce the rate of sedimentation and maximize Mangla benefits, four potential options are theoretically available:

- Manage the distribution of sediments within the reservoir;
- Minimize flow of sediments into the reservoir;
- Maximize evacuation of sediments from the reservoir; and
- Increase the live storage volume of the reservoir.

3.11 Materials and Methods

Landsat-TM data acquired on 09 June 1992 and SPOT-XS acquired on 29 April 2002 were employed in this study. Other materials used were topographic maps (1:50,000). The topographic maps were used for elevation data to generate the DEM, so as to perform a geometric correction of the satellite data.

3.11.1 Geometric correction

Geometric correction of the image was carried out using ER Mapper Software, registering the image to the 1:50,000 scale topographic maps was done by selecting 25 Ground Control Points (GCPs). The Root Mean Square error accepted was less than 1 pixel (20 m) at the first order and the nearest neighborhood transformation. The two corrected scenes were stitched together, and only the study area was clipped with a vector boundary layer.

All scenes were radiometrically and geometrically corrected to a projection system LM1PAK1. Some enhancement techniques were applied to all six scenes to enhance its information. The Landsat-TM data were resampled to 20 meters pixel width so that the data from two different satellites having different spatial resolution (Landsat-TM data has 30 m spatial resolution and SPOT data has 20 m spatial resolution) can be overlayed for comparison. The mosaic of two SPOT scenes was made to cover the wider area of the catchment. Gemetrically corrected and mosaiced SPOT scenes and Landsat scene are shown in Figures 3.2 and 3.3.

3.11.2 Image Enhancement

After geometric corrections and resampling SPOT Xs and Landsat-TM data have gone through different enhancement techniques to get better and enhanced images. Spatial stretch was also applied to digital data for enhancing the effect of siltation in reservoir. Spatially stretched images of Mangla reservoir of 1992 and 2002 are shown in figure, in which the effect of siltation can be seen.

Figure3.2: Rectified Mosaic of two SPOT Satellite Scenes

Figure3.3: Rectified Colour Composite (543) of Landsat Satellite.

3.11.3 Normalized Difference Vegetation Index (NDVI)

NDVI is a useful tool for vegetation detection and estimation. NDVI of SPOT mosaic was done by choosing the band 3 as IR band and band 2 as Red band, while the NDVI of Landsat was run on the false color composite of bands 432, taking band 4 as IR band and band 3 as Red band. The NDVI appears in a pseudo layer, these two pseudo layers were overplayed for forest change detection during 1992 to2002.

3.11.4 Digitization

On the enhanced image different features/objects were identified (using different identification techniques) and digitized in a vector layer using ER Mapper digitization tools. The vector layers of drainage pattern in the catchment area of Mangla reservoir, catchment area's boundary, reservoir boundary for 1992 and 2002 were digitized (for surface area estimation). The digitization of height contours for DEM generation was done by using Digitizer (Cal Comp).

3.11.5 Digital Elevation Model (DEM)

To generate the DEM contour lines at 50ft. intervals for each in hilly areas and in the plains, were digitized using Digitizer (Cal Comp). These data were imported for interpolation by ILWIS software.

ILWIS employs a 3 x 3 weighted moving average window to process group of locations as blocks within a specified search radius. The search radius specifies the distance around each pixel to be interpolated to search for terrain data points, the elevation values of which are used to interpolate the elevation of the former pixel. The weighting function determines how the surface values will be interpolated from the original elevation data points. A Slicing technique was implemented on DEM to get those pixels having height value 1254 feet then draw a line on these pixels. Finally this line is overlaid on the layer of residential areas to get the information about areas that will be effected by increasing Dam's height. From this DEM the Digital Terrain Model (DTM) and 3D grid of Mangla dam's reservoir area was generated for better understanding of the terrain.

Discussion of Results

3.12   Normalized Difference Vegetation Index (NDVI)

NDVI is a useful tool for vegetation detection and estimation. NDVI of SPOT mosaic was done by choosing the band 3 as IR band and band 2 as Red band, while the NDVI of Landsat was run on the false color composite of bands 432, taking band 4 as IR band and band 3 as Red band. The NDVI appears in a pseudo layer, these two pseudo layers were overplayed in two different colors for forest change detection during 1992 to2002. NDVI layer of 1992 Landsat data was displayed in Green layer and that of 2002 SPOT data was displayed in Red layer. These two layers were overlayed, Green and Red colors show change in that particular area and Yellow color shows the permanent features that were present in both 1992 and 2002 data. By using the software we calculated the number of pixels present in each color, thus the area related to the each color. The overlay NDVIs shows that there is more change (red tones) in the areas very near to the reservoir and yellow color in upper part of image show less affected areas in the catchment area. Figure 3.4 shows the pseudo layers of NDVI of both satellites and the overlay of both in different colors.

3.13   Surface area calculation of reservoir

Vector layers of reservoir boundary were sketched using ER Mapper Digitizing tools for both 1992 and 2002. These vector layers were overlayed on the images and reservoir area was clipped and the surface area for both was calculated using ER Mapper calculate statistics wizard. The surface area for 2002 reservoir was found 11163.8 Hectors or 111.63 sq. km. and that for 1992 was19322 Hectors or 193.22 sq. km. This surface area can be used for the water estimation in reservoir in both years. All the drainage pattern in the catchment area of 7200 sq. km. (Area covered by two SPOT scenes), was sketched and marked on the image. This drainage pattern can help us to tell about the terrain of the area that can help us to see where the sources of sedimentation are in the catchment area of Mangla dam. The drainage pattern and reservoir boundaries are shown in Figure 3.5.
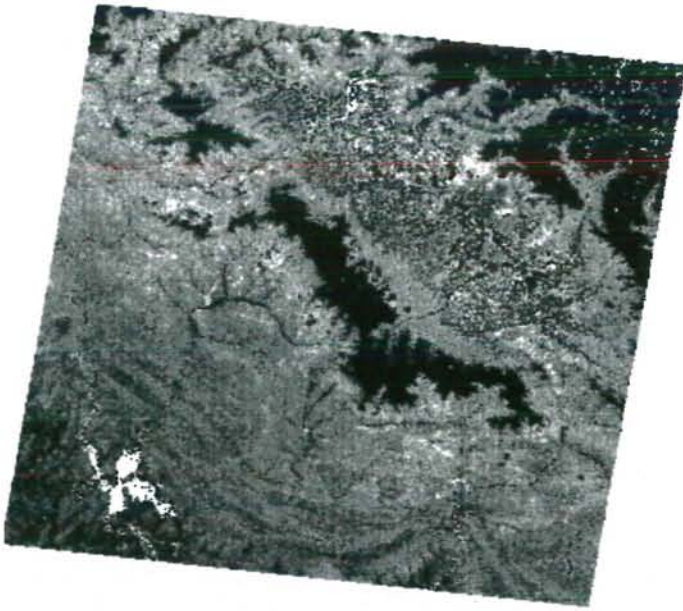
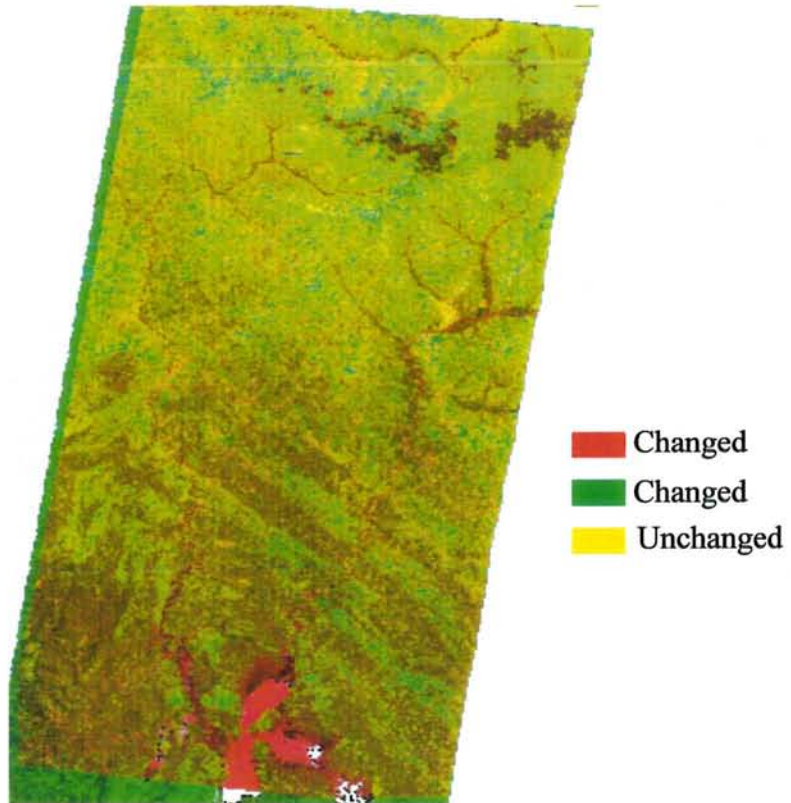Landsat NDVI of 1992

SPOT NDVI of 2002

■ Changed
■ Changed
■ Unchanged

Figure3.4: Merge of Landsat and SPOT NDVI, Shows Changed and Unchanged Areas
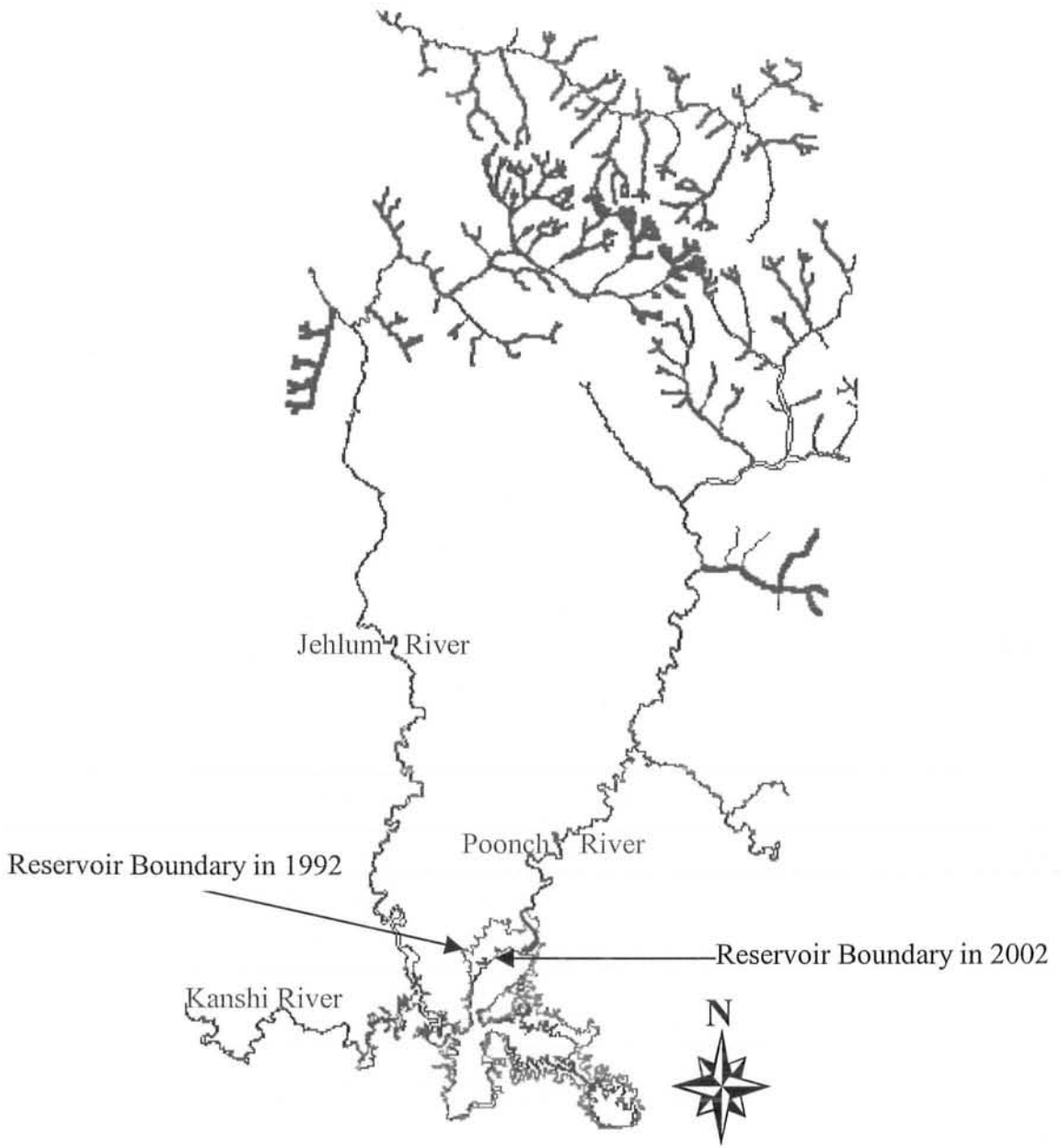from 1992 to 2002 in Mangla Dam's Catchment

Figure3.5: Drainage Pattern in Mangla Dam's Catchment Area and Reservoir Boundary

3.14 Silt Delta

Spatial stretch was applied to digital data for enhancing the effect of siltation in reservoir. Spatially stretched images of Mangla reservoir of 1992 and 2002 are shown in Figures 3.6 and 3.7, in which clear effect of siltation can be seen. From literature we know that the major delta is advancing toward the dam and at present its pivot point is at approx, 5 miles upstream of the Main Dam this delta can be seen very clearly in the Figure 3.6and it was confirmed that the delta is about 4.57 miles upstream the main dam. Area affected by the silt was calculated, and noted that is about 615 sq. acres. in the spatially stretched image of 2002. This calculation shows that the satellite remote sensing is a useful tool for detecting the siltation effects in reservoirs. Although it shows the siltation effects only on the surface and very near to the surface, but it is very useful tool for seeing the siltation effects.

3.15 Environmental Impacts by Raising Dam's Height

As our country require large amount of water to irrigate our fields and we must have sufficient electricity for domestic as well as for industrial purpose. And the storage capacity of reservoir is decreasing because every year a large amount of sediments are deposited in reservoir. Hence an aspect is under consideration, is it feasible to increase the height of dam? if yes then how much storage capacity of the Dam will be increased and what are its effects on the precinct of the Mangla Dam.

3.15.1 Generation of DEM

The output digital elevation model (DEM) was a 16-bit single band raster image as the interpolated elevation. Each pixel's value represented the elevation at that point. The output was evaluated by randomly selecting some sample points from the interpolated DEM, and comparing the interpolated values with corresponding points in the topographic map. This correlation provides a measure of spatial correlation and spatial association between two variables [9]. A linear association was observed between interpolated elevation and real topographic elevation values.
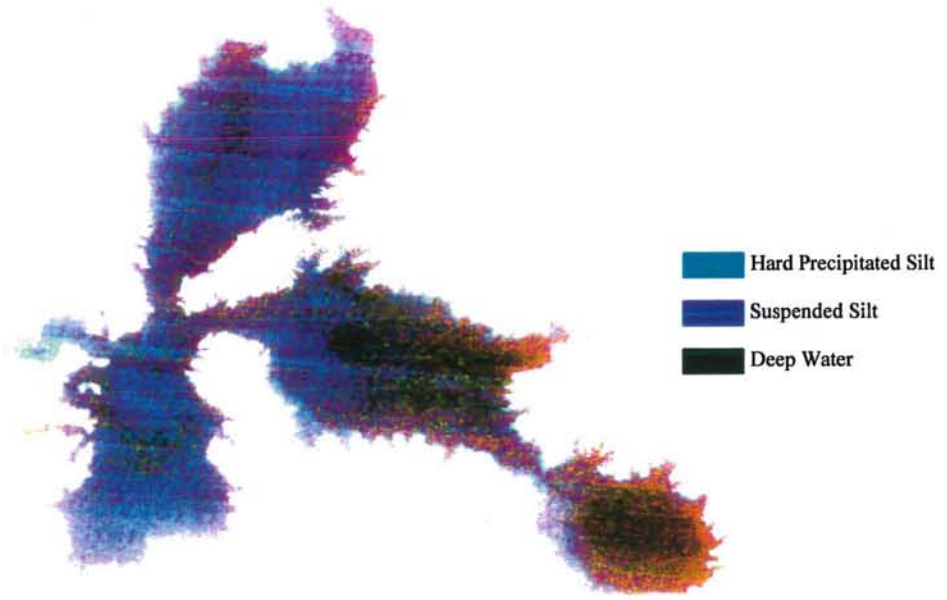
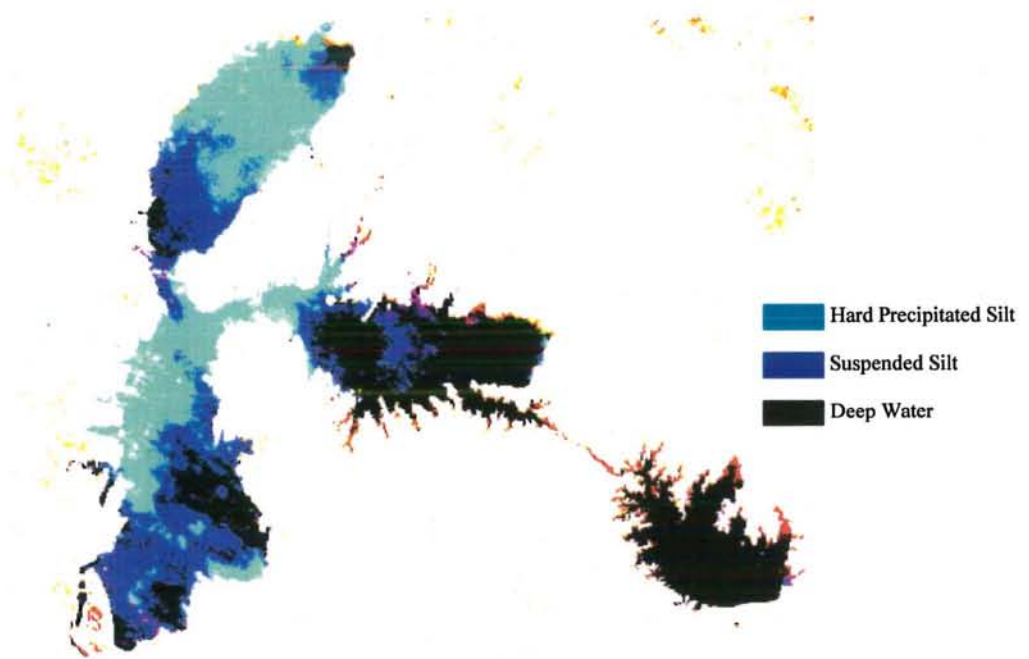**Figure3.6**: Spatially stretched image for Silt, of Mangla reservoir in1992

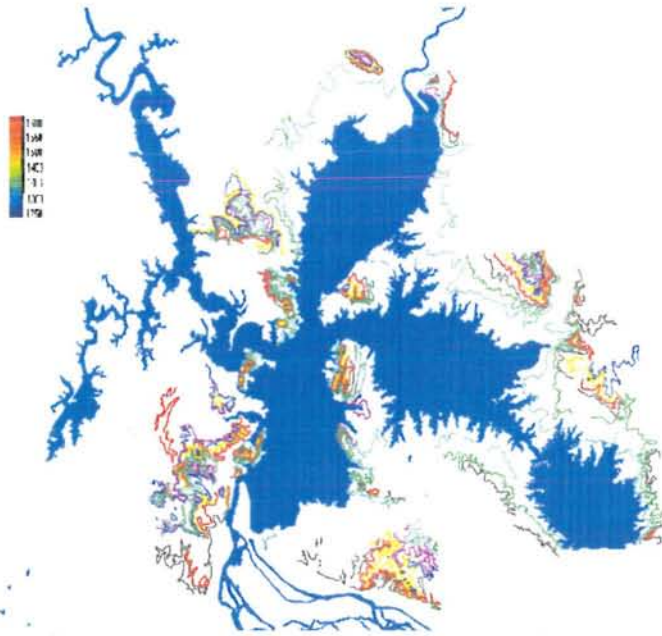**Figure3.7**: Spatially stretched image for Silt, of Mangla reservoir in 2002

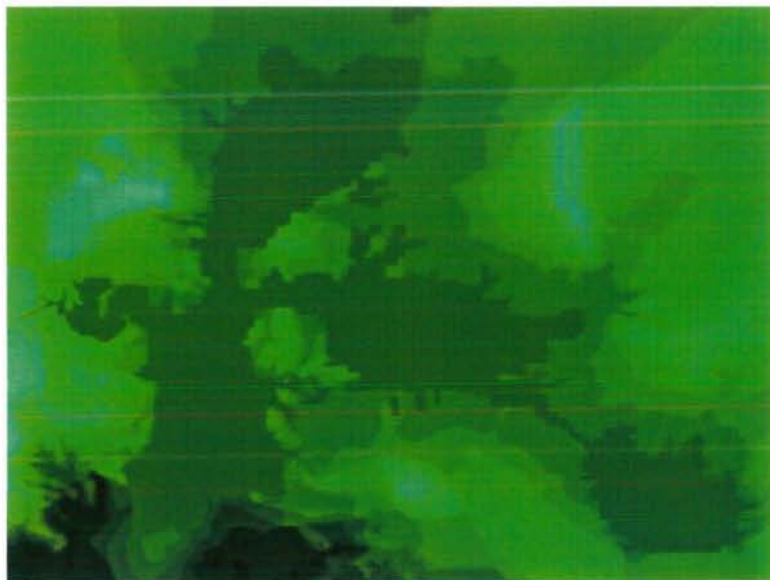**Figure3.8:** Height contours of the area

Figure3.9: DEM of Mangla Dam, shades of green color from light
to dark represents high altitude to low altitude respectively i
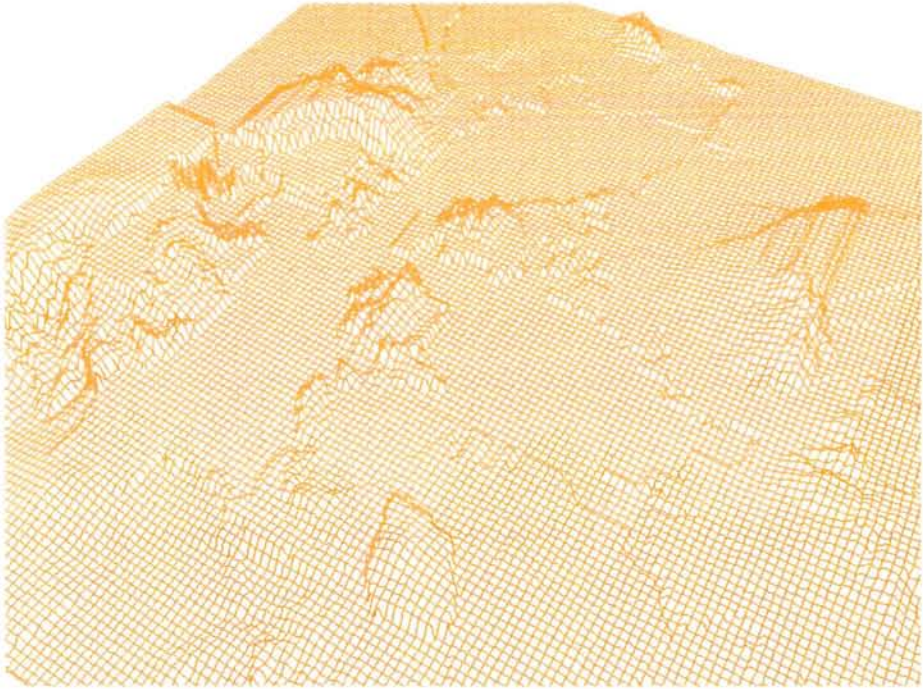the surrounding of Mangla dam

Figure3.10: 3-D Grid of the area

Figure3.11: DTM of the Mangla, Landsat image is overlaid on the DEM of Mangla

The 16-bit DEM was rescaled to 8-bit raster so that it was compatible with that used for Landsat-TM. A Slicing technique   was implemented on DEM to get those pixels having height value 1254 feet then draw a line on these pixels. Finally this line is overlaid on the layer of residential areas to get the information about areas that will be affected by increasing Dam's height. Figure3.12 shows the total affect of Dam's height raising, Blue is the Proposed Extent of the Reservoir and the sky blue is the existing level of the reservoir. Red patches existing on the blue are those residential areas, which will effect by the water

After getting DEM the image was overlaid on DEM to get the DTM of the Mangla dam. DEM and DTM are shown in Figures 3.8, 3.9, 3.10 and 3.11.

3.15.2 Calculation of Results:

The project's 80% objectives have been achieved; rest of the work is not completed due to unavailability of different maps and ground truth information. In spite of many difficulties and problems the following conclusions have been drawn.

- ➤ The existing surface area of Mangla Reservoir is 193.22 Sq km
- ➤ After increasing the dams height the Surface area of the reservoir will be 245.116958 Sq km.
- ➤ About 1557493 Sq m residential area will be affected by the rising of the Dams height.
- ➤ Forest surrounding the reservoir will also be affected; this causes the destruction of many types of trees, herbs & other vegetation, and animal species will also be disturbed.
- ➤ A large cultivated area will be degraded.

Note: These results are preliminary and need to be verified by ground truth information and other data.
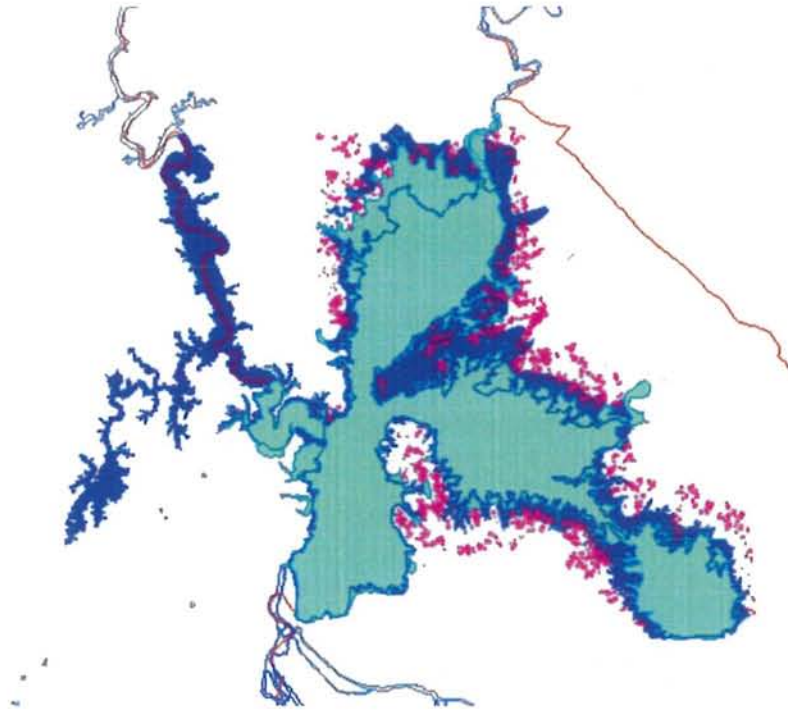
Figure 3.12: Blue is the Proposed Extent of the Reservoir and the sky
blue is the existing level of the reservoir. Red patches
existing on the blue are those residential areas, which will
effect by the water.
Existing reservoir water level is 1210 feet and proposed
will be 1254 feet

3.16 CONCLUSIONS

This study illustrates the application of SRS, DEM and GIS for monitoring a watershed. The case of the Mangla Dam illustrates the use of high-resolution satellite data, Landsat TM, and SPOT through digital image processing techniques. This can be combined using DEM, derived from reliable data and maps on land use. GIS technology can be employed to create DEM, and to map the change detection. The interfacing of GIS, DEM and SRS in this study provided a new and exciting capability to analyze the dynamics of land-use change and to assess changes in residential areas and vegetation in the landscape after raising the Dam's height. Regardless of the accuracy of results achieved, Which can be improved through ground truth surveys, image analysis techniques used in this study, have been found helpful in identification of temporal changes in the reservoir. The results obtained by this study, thus provide encouragement for achieving more confident results in future.

Furthermore, the integration of SRS and GIS is a very useful technique for land capability and suitability classification, and in planning new alternative land use options.

Bibliography

1. Nicholas M. Short, Sr, *"NASA Remote Sensing Tutorial"* New Yok, USA.

2. Guneriussen, T. and H. Johnsen *"NASDA Remote Sensing Tutorials"*.

3. ERDAS. 1991. *ERDAS Field Guide*. Second Edition, ver. 7.5. Erdas, Inc., Atlanta, USA.

4. Campbell, J.B. 1987. *Introduction to Remote Sensing*. Guidford, New York.

5. N.K. Siddiqui, Remote Sensing for Prediction of Floods in Jehlum River in Pakistan and The Significance of Kashimir Valley- The Pir Panjal Deppression, *GEOSAS-III*, Lahore Pakistan. 23-26 September 2000.

6. WAPDA, Sendimentation of Mangla Reservoir, *Hyderographic Survey 2000*.

7. Integration Of Geographic Information Systems (GIS) And Satellite Remote Sensing (SRS) For Watershed Management, *Apisit Eiumnoh School of Environment, Resources and Development Asian Institute of Technology P.O. Box 4, Klong Luang, Pathumthani 12120, Thailand*.

8. Lillesand, T.M. and R.W. Kiefer. 1994. *Remote Sensing and Image Interpretation*. (3rd Edition). John Wiley and Sons, Singapore.

9. Haining, R. 1990. *Spatial Data Analysis in the Social and Environmental Sciences*. Cambridge University Press, Cambridge, United Kingdom.

10. FEP Atlas,1993; Published by Eastern Publications.